AFRL-AFOSR-VA-TR-2016-0179

CREATING SPACE PLASMA FROM THE GROUND

Herbert C Carlson
UTAH STATE UNIVERSITY

05/12/2016
Final Report

Air Force Research Laboratory
AF Office Of Scientific Research (AFOSR)/ RTB1
Arlington, Virginia 22203
Air Force Materiel Command

REPORT DOCUMENTATION PAGE

Form Approved
OMB No. 0704-0188

PLEASE DO NOT RETURN YOUR FORM TO THE ABOVE ORGANIZATION.

1. REPORT DATE *(DD-MM-YYYY)*	2. REPORT TYPE	3. DATES COVERED *(From - To)*
05/14/2016	Final	08/14/2012-05/14/2016

4. TITLE AND SUBTITLE
Creating space plasma from the ground

5a. CONTRACT NUMBER

5b. GRANT NUMBER
FA9550-11-1-0236

5c. PROGRAM ELEMENT NUMBER

6. AUTHOR(S)
Herbert C. Carlson

5d. PROJECT NUMBER

5e. TASK NUMBER

5f. WORK UNIT NUMBER

7. PERFORMING ORGANIZATION NAME(S) AND ADDRESS(ES)
Utah State University/CASS

8. PERFORMING ORGANIZATION REPORT NUMBER

9. SPONSORING/MONITORING AGENCY NAME(S) AND ADDRESS(ES)
AFOSR

10. SPONSOR/MONITOR'S ACRONYM(S)

11. SPONSOR/MONITOR'S REPORT NUMBER(S)

12. DISTRIBUTION/AVAILABILITY STATEMENT
Public open distribution

13. SUPPLEMENTARY NOTES
NA

14. ABSTRACT
It was predicted (Carlson, 1987; 1993) that once HF radio waves achieved ionospheric energy densities comparable to that from the solar EUV, they could produce their own ionosphere. That work estimated a GW ERP of rf energy would produce an ionosphere half that from an overhead sun, assuming ~15% efficiency conversion of rf energy to accelerated electron energy. [Until 2009 only one experimental estimate existed, ~15% from Carlson, 1982.] The production mechanism proposed was impact ionization, by HF-accelerated electrons, to energies exceeding thermospheric ionization potentials. Solar EUV, aurora, and high-power HF radio-waves produce suprathermal electrons in the 15-100 eV energy range, yielding long-lived ionization in the ionosphere. Once suprathermal electrons are produced, the Aeronomy of production, transport, and recombination are in common. The key to understanding artificial ionization thus reduces to conversion efficiency of HF energy to ionization. By 2008 technology reached ~GW ERP. The prediction was tested, and confirmed [Pedersen et al, 2009, Blagoveschenskaya et al, 2009] at high latitudes. However, confirmation was at only high latitudes, and by then new theory [Gurevich, Zybin, and Carlson, 2005] had shown multiple

15. SUBJECT TERMS
Space plasmas
plasma instabilities
artificial ionospheres

16. SECURITY CLASSIFICATION OF:			17. LIMITATION OF ABSTRACT	18. NUMBER OF PAGES	19a. NAME OF RESPONSIBLE PERSON
a. REPORT	b. ABSTRACT	c. THIS PAGE			Herbert C. Carlson
U	U	U	UU	40	19b. TELEPHONE NUMBER *(Include area code)* 1 435 760 1831

Reset

INSTRUCTIONS FOR COMPLETING SF 298

1. REPORT DATE. Full publication date, including day, month, if available. Must cite at least the year and be Year 2000 compliant, e.g. 30-06-1998; xx-06-1998; xx-xx-1998.

2. REPORT TYPE. State the type of report, such as final, technical, interim, memorandum, master's thesis, progress, quarterly, research, special, group study, etc.

3. DATES COVERED. Indicate the time during which the work was performed and the report was written, e.g., Jun 1997 - Jun 1998; 1-10 Jun 1996; May - Nov 1998; Nov 1998.

4. TITLE. Enter title and subtitle with volume number and part number, if applicable. On classified documents, enter the title classification in parentheses.

5a. CONTRACT NUMBER. Enter all contract numbers as they appear in the report, e.g. F33615-86-C-5169.

5b. GRANT NUMBER. Enter all grant numbers as they appear in the report, e.g. AFOSR-82-1234.

5c. PROGRAM ELEMENT NUMBER. Enter all program element numbers as they appear in the report, e.g. 61101A.

5d. PROJECT NUMBER. Enter all project numbers as they appear in the report, e.g. 1F665702D1257; ILIR.

5e. TASK NUMBER. Enter all task numbers as they appear in the report, e.g. 05; RF0330201; T4112.

5f. WORK UNIT NUMBER. Enter all work unit numbers as they appear in the report, e.g. 001; AFAPL30480105.

6. AUTHOR(S). Enter name(s) of person(s) responsible for writing the report, performing the research, or credited with the content of the report. The form of entry is the last name, first name, middle initial, and additional qualifiers separated by commas, e.g. Smith, Richard, J, Jr.

7. PERFORMING ORGANIZATION NAME(S) AND ADDRESS(ES). Self-explanatory.

8. PERFORMING ORGANIZATION REPORT NUMBER. Enter all unique alphanumeric report numbers assigned by the performing organization, e.g. BRL-1234; AFWL-TR-85-4017-Vol-21-PT-2.

9. SPONSORING/MONITORING AGENCY NAME(S) AND ADDRESS(ES). Enter the name and address of the organization(s) financially responsible for and monitoring the work.

10. SPONSOR/MONITOR'S ACRONYM(S). Enter, if available, e.g. BRL, ARDEC, NADC.

11. SPONSOR/MONITOR'S REPORT NUMBER(S). Enter report number as assigned by the sponsoring/ monitoring agency, if available, e.g. BRL-TR-829; -215.

12. DISTRIBUTION/AVAILABILITY STATEMENT. Use agency-mandated availability statements to indicate the public availability or distribution limitations of the report. If additional limitations/ restrictions or special markings are indicated, follow agency authorization procedures, e.g. RD/FRD, PROPIN, ITAR, etc. Include copyright information.

13. SUPPLEMENTARY NOTES. Enter information not included elsewhere such as: prepared in cooperation with; translation of; report supersedes; old edition number, etc.

14. ABSTRACT. A brief (approximately 200 words) factual summary of the most significant information.

15. SUBJECT TERMS. Key words or phrases identifying major concepts in the report.

16. SECURITY CLASSIFICATION. Enter security classification in accordance with security classification regulations, e.g. U, C, S, etc. If this form contains classified information, stamp classification level on the top and bottom of this page.

17. LIMITATION OF ABSTRACT. This block must be completed to assign a distribution limitation to the abstract. Enter UU (Unclassified Unlimited) or SAR (Same as Report). An entry in this block is necessary if the abstract is to be limited.

Final Report (2016)
Creating Space Plasma from the Ground

Grant FA9550-11-1-0236 AFOSR Program Manager Dr. Kent Miller

PI: Herbert C. Carlson
Center for Atmospheric and Space Sciences, Utah State University, Logan, UT 84322

Abstract:
It was predicted (Carlson, 1987; 1993) that once HF radio waves achieved ionospheric energy densities comparable to that from the solar EUV, they could produce their own ionosphere. That work estimated a GW ERP of rf energy would produce an ionosphere half that from an overhead sun, assuming ~15% efficiency conversion of rf energy to accelerated electron energy. [Until 2009 only one experimental estimate existed, ~15% from Carlson, 1982.] The production mechanism proposed was impact ionization, by HF-accelerated electrons, to energies exceeding thermospheric ionization potentials. Solar EUV, aurora, and high-power HF radio-waves produce suprathermal electrons in the 15-100 eV energy range, yielding long-lived ionization in the ionosphere. Once suprathermal electrons are produced, the Aeronomy of production, transport, and recombination are in common. The key to understanding artificial ionization thus reduces to conversion efficiency of HF energy to ionization. By 2008 technology reached ~GW ERP. The prediction was tested, and confirmed [Pedersen et al, 2009, Blagoveschenskaya et al, 2009] at high latitudes. However, confirmation was at only high latitudes, and by then new theory [Gurevich, Zybin, and Carlson, 2005] had shown multiple physical processes conspire to significantly amplify high latitude suprathermal electron production. To test if the prediction was therefore invalidated at mid-latitudes, we performed a definitive test at Arecibo in November 2015, its first HF operation since Hurricane George in 1998. We developed a theoretical framework, performed a unique experiment, did major improvements in measurements, and measured comparable HF and solar suprathermal electron production rates, thereby confirming the 1993 prediction.

1. Introduction: It was predicted (Carlson, 1987, 1993) that once high-power HF transmitters reached Giga-Watt ERP (effective radiated power) levels, they would surpass probing/perturbing Earth's ionosphere, and become capable of creating an ionosphere from the ground (Figure 1). A National Academy of Sciences report [ISBN 978-0-309-29859-9] featured this figure 1 herein below as its motivational figure S.3 ["Hierarchy of heater effective radiative thresholds for excitation of plasma processes in the lower atmosphere. SOURCE H. C. Carlson, Jr., High-Power HF modification: Geophysics, span of EM effects, and energy budget, Advances in Space Research, 13:15-24, doi:10.1016/0273-1177(93)90046-E, 1993. Courtesy of Herbert Carlson and COSPAR."]

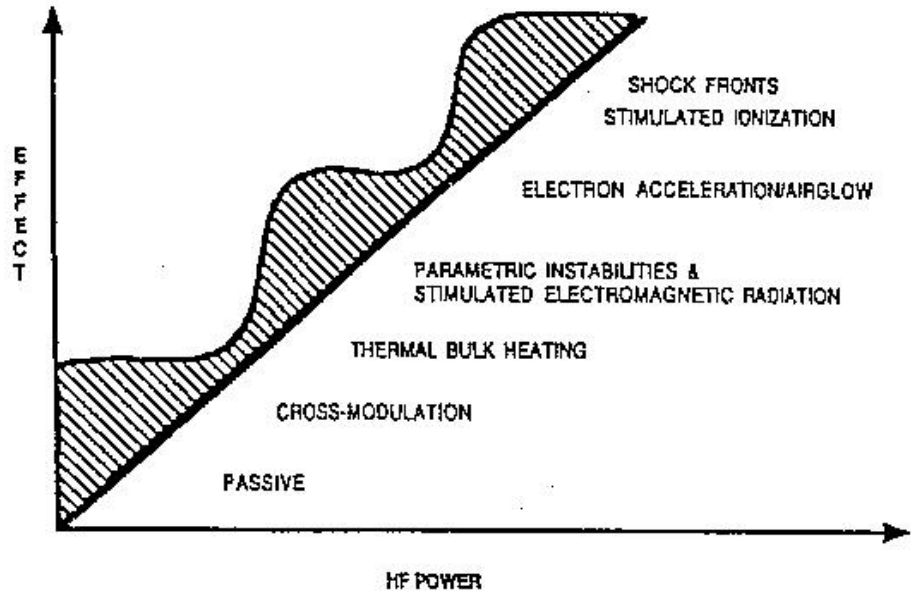

Figure 1: As HF power is steadily increased, the ionospheric response changes discontinuously, revealing its non-linear response as subsequent plasma instability thresholds are passed. Based on study of HF driven parametric instabilities and electron acceleration at the Arecibo Observatory (1993) both qualitatively illustrated that nonlinearity with this figure, and quantitatively predicted the stimulated ionization threshold to be about 1 GW ERP. [Carlson, 1993]

That prediction was verified in 2010, at both the HAARP AK HF heating facility (where this PI was present for running the experiment with Todd Pedersen) (Pedersen et al, 2009, 2010), and the EISCAT Tromso HF heating facility (Blagoveshchenskaya et al, 2009). Both landmark publications included (this PI) Carlson as coauthor of these experimental confirmations of his prediction.] Figure 2 illustrates the most direct confirmation (Pedersen et al, 2010) of these.

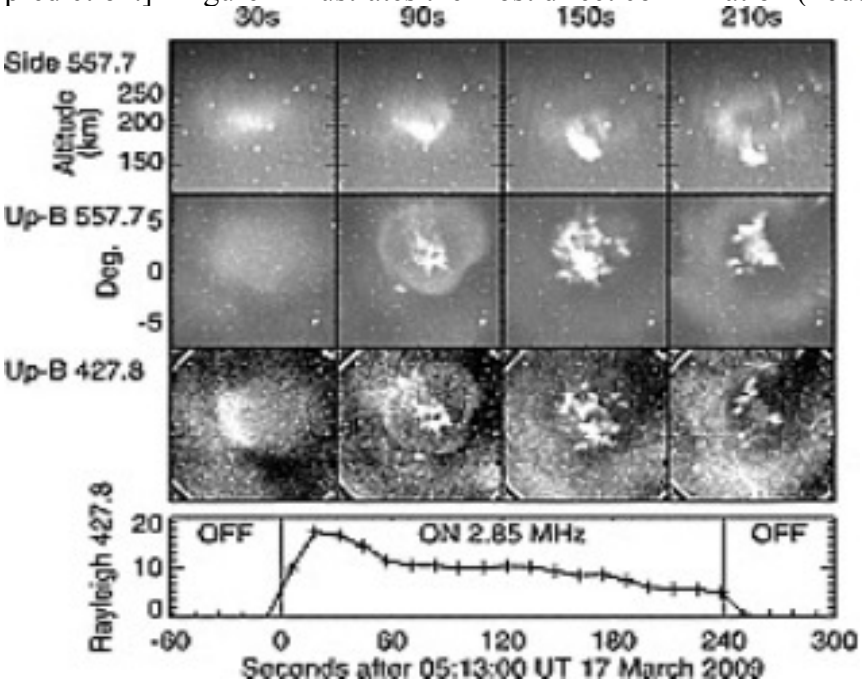

Figure 2: (Top left, figure 2a): Top row of four frames- side-view images of artificial optical 557.7 nm emissions as viewed from a remote site (with altitudes along the HAARP field line indicated); images of artificial optical emissions as viewed looking upwards along the magnetic field line from the HAARP site with high resolution at 557.7 nm (2nd row of frames) and 427.8 nm (3rd row of frames). Average calibrated intensities at 427.8 nm for the central region of the images are shown in the 4th row as a function of seconds after the transmitter turned on at 5:13:00 UT.

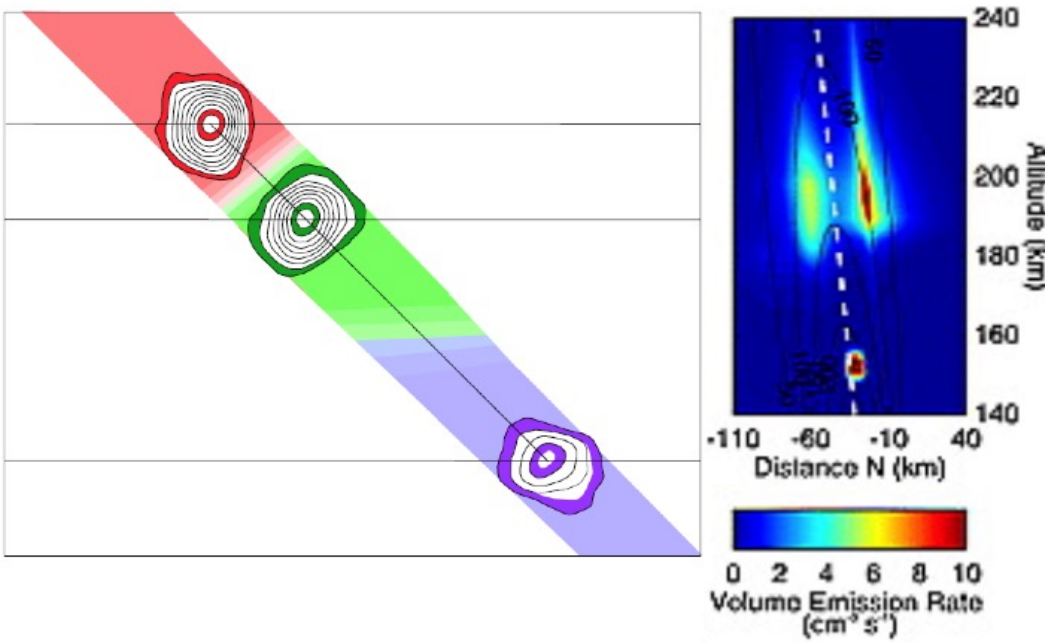

Figure 3. Right: The 557.7 nm images of figure 2, for 210 second after HF turn on, have been combined using a tomographic algorithm to provide a cross-section of the optical volume emission rate (false color scale) in the magnetic meridian plane. The HAARP magnetic field line has been superimposed on the tomographic cross section. Left: data from the Arecibo Observatory, April 20, 1988, 02:25-02:27 AST, illustrating for the first time (Carlson and Jensen, 2014) the depth of penetration dependence on wavelength of optical emission [630.0 nm in red, 557.7 nm in green, 777.4 nm in blue].

The two 2009 confirmations at high latitudes, involve fundamentally different physics than at lower mid-latitudes. Proof at both mid and high latitudes is required for understanding the physics relevant to Earth's space environment.

The essential physics for realization is to convert HF electromagnetic (EM) into an ionizing form of energy. This was hypothesized and confirmed to be by acceleration of ambient electrons to of supra-thermal energies via acceleration driven by HF excited plasma instabilities. At high latitudes such as HAARP that physics includes two critical steps: (1) plasma-structuring processes [including trapping of the HF EM energy for nearly complete deposition into the ionospheric plasma], and (2) a resonance matching condition that amplifies efficient plasma-instability conversion of the radio frequency energy into electron acceleration. At low latitudes such as Arecibo, trapping is not possible, and creation of supra-thermal electrons is by a different class of plasma instabilities. At these latitudes only one pass of the HF wave through the plasma is available to deposit energy into ionization production. While high vs. mid latitudes have

major differences for the steps leading up to supra-thermal electron production, they share dominant commonalities for the physics of the subsequent steps, in which accelerated electrons must be transported from their acceleration region to where their collisions with neutrals yield ionization. At high altitudes near or above ~250 km, this can be many neutral scale heights; near or below 200 km the production can be nearly local.

To resolve the elements of this challenge we have developed an energy budget approach that we lay out below. This approach enables good estimates of ionization production rates, and defines a framework within which experiments can be performed to test [pass or fail] that framework for understanding the creation of space plasma using high HF transmitters. The experiments we designed and implemented, interpreted in this framework, support the conclusion of inevitability of a capability to make artificial ionization competitive with solar-produced, when guided by the principles outlined below.

In the course of contrasting high vs. mid-latitudes, we explain the two new measurement techniques we have developed to extend the Arecibo capability in HF heating diagnostics.

2. Background

2.1 Scientific Background

The ionosphere, a conducting shell enveloping Earth, was discovered in a search to explain the success of the bold experiment for which Marconi won the 1906 Nobel Prize, in successful trans-Atlantic wireless transmission of HF radio signals. The ionosphere has since been widely studied by radio wave remote sensing techniques, in situ measurements on rockets and satellites, facilitated by key optical techniques. Early experiments used weak HF radar transmissions to sense and monitor its behavior, to passively probe its properties. Since 1971 it has been possible to use higher-power HF transmissions to perturb its properties [test the system as a black box in the lab by input-response techniques], using power densities approaching those of the ambient electron gas that could thereby be perturbed. Perkins et al, 1974 noted parametric instabilities.

It was predicted (Carlson, 1987, 1993) that once high-power HF ionospheric modification facilities achieved ~GW ERP, they would not merely modify preexisting, but produce new ionospheric ionization significant relative to that from the sun. That prediction was based on calculating the power density needed to approximate that of the Sun producing the natural ionosphere, and by further identifying a mechanism that would convert HF EM energy into a form of ionizing energy. Key to doing so was to estimate the fraction of EM energy that could be so converted. Within two decades of that prediction, HF technology has recently passed that projected ERP threshold at high latitudes, and the PI on this grant teamed with colleagues to produce experimental evidence of confirmation of that prediction (Blagoveschchenskaya et al., 2009, Pedersen et al. 2009, 2010).

The only experiment at mid-latitudes however was the single measurement (Carlson et al, 1982) on which the original prediction was based. That experiment had never been repeated/verified, and when Hurricane George destroyed the Arecibo HF Heating facility in September 1998, confirmation had to await reconstruction completed in November 2015. During the intervening interval many important advances occurred in measurement and theory. Here we update the physics supporting the ~two decade-old prediction, including those theoretical/experimental

developments of significance to its quantification, and closely examine the evidence for creation of ionospheric plasma from the ground. That is the purpose of this work.

The steps to go through are: 1) define the HF ERP needed to deliver enough EM energy density to ionospheric altitudes to produce ionization of significance when compared with that from the sun; 2) identify what mechanism converts that HF EM energy into an ionizing form of energy (we now know accelerated electrons can do the job); 3) find the mechanism that enables the HF energy to reach the altitude where acceleration processes occur (vs. energy scattering or dissipation to merely thermal electron gas heating); 4) demonstrate where the ionization is produced relative to the altitude of HF instability interactions; and 5) search for mechanisms that enhance/maximize the efficiency with which the HF energy leads to accelerated electrons. Within this context we then must examine data collected to test for artificial ionization produced from the ground (demonstrate the effect is real), and then look for evidence supporting the candidate theoretical framework proposed here.

Below we present a framework facilitating understanding of how to create space plasma from the ground, and for application of this capability to: aeronomy, chemistry, space sciences, radio propagation, and for application to radio propagation modes this enables.

2.2 Historical Background

The first serious high-power ionospheric modification research to appear in the open literature was initiated in Plattville, CO (Utlaut and Cohen, 1971; Radio Science Special Issue, vol 9, 1974). Findings were based on HF heater-induced airglow, spread-F and wide-band field-aligned ionization structure, and wide-band absorption. Work soon after at the Arecibo Observatory added measurements of profiles of plasma temperature heating and electron density redistribution (Gordon et al, 1971, Gordon and Carlson, 1974), as well as the experimental discovery that HF power densities sufficiently great to enhance the bulk electron gas temperature have associated electric fields sufficient to drive instabilities in the space plasma (Carlson, Gordon and Showen, 1972). Increasing the plasma bulk temperature can vertically redistribute bulk plasma density profiles; instabilities can lead to plasma structuring and also acceleration of a small fraction of the electron population leading to impact excitation of optical emissions in the upper atmosphere (Sipler et al., 1972; Haslett and Megill, 1974). Observations of HF-excited 630.0 nm and 557.7 nm optical enhancements were common, with the 557.7 nm playing the key role of providing evidence of accelerated electron impact excitation by electrons of energy above 4 eV. 630.0 nm has such a low excitation threshold (1.96 eV) that electrons in the thermal distribution can give detectable emission for electron gas temperatures (Te) exceeding about 2500 K, though Arecibo measured much lower Te.

Prevailing theory at that time (Fejer, 1977, 1979) said acceleration of electrons (thermal energy ~0.1-0.2 eV) could not exceed a few eV, far below the threshold for production of ionization. An incoherent scatter radar technique proved that theory to be wrong by 1972, by observing electrons accelerated to energies sufficient to produce ionization (Carlson et al, 1982). That publication went on to explain that by adding the physics of aeronomy to the earlier plasma physics, leading to adding elastic scattering of accelerated electrons, would allow an electron multiple passes through the electron acceleration region to reach much higher energies than theory previously gave. HF-excited plasma waves can transfer energy to electrons by the landau damping mechanism, with local acceleration experienced as the electrons cross cavitons, now able to have multiple passes vs. a single pass through the acceleration region. This more

complete physics was inserted into the quantitative theory by Gurevich et al (1985), to allow more realistic modeling.

It is now well accepted that a fraction of the rf energy delivered to near-earth space excites plasma instabilities, which accelerate ambient electrons to energies in excess of the ionization threshold for upper atmospheric atoms and molecules. Ambient electrons of thermal energy ~0.1 eV are heated to thermal energies a few times this, by natural solar-driven processes by day, and also by deviative absorption of rf energy incident from ground-based HF heating experiments. Electrons in the tail of this distribution are also accelerated to energies ~100 times their thermal energy by plasma instability processes. We have seen proof of electron acceleration by impact excitation of optical emissions and other means, to energies in excess of several energy thresholds: 2 eV (630.0 nm emissions), 4 eV (557.7 nm emissions), 9 eV (rocket borne electron spectrometer-Rose et al, 1985), 11 eV (777.4 nm emission), 19 eV (391.4 nm emission), and 25 eV (incoherent scatter plasma-line spectra). The ionization potential of atomic oxygen (O+), molecular nitrogen (N_2) and molecular oxygen (O_2) is respectively 13.62 eV, 15.58 eV, and 12.06 eV, which lines have been observed (Bernhardt et al., 1989; Pedersen et al., 2003, Carlson and Jensen, 2014; Kosch et al., 2000; Gustavsson et al., 2005).

The one existing quantitative prediction (Carlson, 1993; Carlson, 1987) that a significant amount of space plasma could be produced from the ground sets the threshold for such capability, as once HF radar technology realized GW ERP levels. That quantitative prediction was based on comparison of the HF power density that could be delivered to the F-region space plasma environment relative to that from the sun, which produces our natural ionosphere. From e.g. Rishbeth and Garriott (1969), an overhead sun for average solar conditions (sun spot # ~60) leads to an electron production rate of ~10^3 cm^{-3} s^{-1} in the ionospheric F-region peak, which, spread over ~100 km (two atomic oxygen scale heights), gives a column ionization rate of ~10^{10} ionizations cm^{-2} s^{-1} columnar rate. For ~30eV per ionization by electron impact ionization this represents 3 10^{11} eV cm^{-2} s^{-1} = 4 10^{-8} Watts cm^{-2}. A GWatt ERP class HF facility would deliver ~1.3 10^{-7} Watts cm^{-2} to ~250 km altitude.

At the time the only available experimental value for efficiency of conversion of HF to accelerated electron energy was that reported by Carlson et al (1982), ~15%, which, if extrapolated from that experimental 100 MW ERP to a GW, would lead to about half the production rate of an overhead sun. The validity of this prediction hinged on extrapolation of physics to future higher power densities. Carlson (1987, 1993) presented evidence indicating that significant ionization not only could but also should be expected to happen.

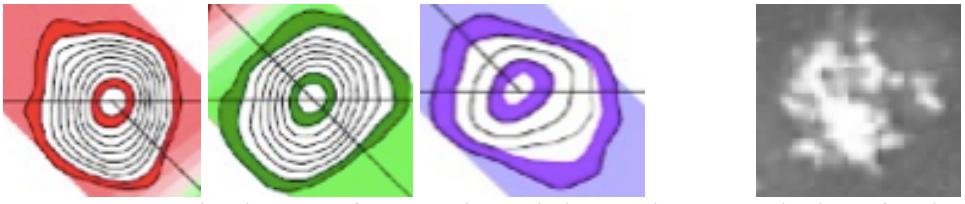

Figure 4. Contrasting images of HF accelerated electron impact excitation of optical emissions, at lower latitudes (e.g. Arecibo) vs. higher latitudes (e.g. HAARP). a) The three colored images, left to right are respectively 630.0 nm, 557.7 nm, and 777.4 nm electron impact excited emissions looking vertically upwards over Arecibo filling the full HF beam. b) Grey and white image to far right is 557.7 nm emission seen vertically over HAARP, filing the magnetic zenith effect portion of the HF heater beam. All images are 2 to 2.5 minutes after HF turn-on. At Arecibo no structuring could be detected at any granularity or degree of spatial smoothing, typical of low to mid latitude conditions. The spatial

structuring in the HAARP is typical of its high latitude location. This contrast is one of the more salient manifestations of the *different effects* driven by the *different physics* dominating HF heating al low (Carlson et al, 1972) vs. high latitudes (Gurevich et al, 2001, 2002).

3. Context

3.1 Fraction of HF energy deposited in ionosphere

Five key successive steps of progress between 1995 and 2001 led to the foundation of learning to deposit significant fractions of radiated HF energy into the ionospheric plasma. (1) A key step was recognition that excitation of upper hybrid (UH) waves simultaneously led to excitation of plasma striations on scales of meters and above. More quantitatively, in the first step (Gurevich, Zybin, and Lubyanov, 1995) showed that a steady state of isolated striations developed during ionospheric modification by high-power HF radio waves, in which the electron gas would be heated to 2-4 times its initial thermal value, and electron plasma density (n_e) depletions would saturate a few to ~10%. (2) Because the perturbation in n_e is always negative (Gurevich et al, 1997), this leads to parametric decay of upper hybrid waves becoming trapped inside the n_e depletions, self-focusing on striations. It is nonlinear because as the HF pump electric field (E_p) increases, it increases the n_e depletions, further focusing the incident E_p into the depletions, and so on leading to the nonlinear cycle on an increasing number of striations. (3) Focusing increases the effective E_p, which increases the number of striations, producing bunches of striations (Gurevich et al, 1998), large-scale structures 100s m, containing m-scale striations. (4) Because bunches (larger scale structures) have only depleted n_e, HF waves can be trapped (Gurevich et al, 1999). The trapping is most effective only for conditions where the pump HF wave is propagating sufficiently close to parallel to earth's magnetic field B. (5) The geometry of the trapped region was quantified by Gurevich, Carlson and Zybin (2001) to be in an oval region towards magnetic south of the HF transmitter site. The only available data available initially to search for such effect was the Arecibo April 20, 1988 data shown in this paper, which should have been too far from parallel propagation for an effect to show, and which as anticipated verified no effect within the limits of measurement (small fraction of a percent). The effect was soon confirmed when data became available from HAARP (Pedersen and Carlson, 2001; Gurevich, Zybin, Carlson, and Pedersen, 2002).

3.2 Electron transport model.

We first needed to focus on developing analysis tools for interpretation of data to be taken at the upcoming HF heating experiment in Arecibo, as well as of key data taken in the past. This relates to a theoretical model for suprathermal electron transport, energy exchange, and excitation of both optical emissions and of plasma waves to understand electron acceleration processes in high intensity HF radiation fields.

There has been considerable preparation for the first HF heating experiment at Arecibo since the time the hurricane destroyed the earlier HF facility, and after over a decade of waiting this upgraded facility is planned to operate in early 2014. The incoherent scatter radar diagnostic will provide major experimental support for daytime or nighttime operations, in addition to optical sensor support in darkness.

The (ISR) incoherent scatter spectrum (Evans, 1969) arising from the ionosphere has two major components. The ion line component from ion-acoustic waves has been used extensively for aeronomical research. The much weaker electron component, or plasma line, has been used less

extensively. The plasma line component gives information about the energy stored in Langmuir waves, which have frequencies near the local plasma frequency. Such waves are always present at a very low "thermal level" in the ionosphere because of self-interaction among thermal electrons.

When photoelectrons are present in the plasma these waves are substantially enhanced by wave-particle interactions [Perkins and Salpeter, 1965; Yngvesson and Perkins, 1968- henceforth YP]. Photoelectrons streaming through the ionosphere generate Cherenkov emissions of Langmuir waves that greatly enhance thermal Langmuir wave amplitudes and the corresponding strength of the plasma line. The Langmuir wave amplitude is controlled by the amount of time that the photoelectrons spend near the same phase region as the Langmuir wave train; this promotes energy transfer to the Langmuir wave. Thus, the plasma wave intensity depends on the electron velocity distribution function. YP have expressed the energy in the waves in terms of an apparent plasma temperature $T_p(E\phi)$ or intensity $kT_p(E\phi)$ given by:

$$kT_p = kT_e \frac{f_m(E_\phi) + f_p(E_\phi) + \chi}{f_m(E_\phi) - kT_e \frac{df_p(E_\phi)}{dE_\phi} + \chi} \qquad (1)$$

where $\mathbf{f}_p$ is the one-dimensional velocity distribution of the photoelectrons along the radar wave vector; $\mathbf{f}_m$ is a modified one-dimensional Maxwellian velocity distribution of the ambient electrons.

Application of plasma line techniques to estimate suprathermal electron fluxes in the ionosphere, and their limitations, have been carefully examined in the literature (Cicerone et al, 1973, Cicerone 1974). Carlson et al (1977) have demonstrated a new technique for extracting information about the photoelectron and/or suprathermal electron spectrum from ISR plasma line data, with minimum ambiguity. We have pursued re-enabling that new technique here, under this grant, by recovering and updating/upgrading early work by Mantas (1973, 1975a) and Mantas et al (1975b, 1978). Part of the update/upgrade has included reexamination of latest electron collision cross-sections (Dalgarno, A. and G. Lejeune (1971); Pavlov (1998a, 1998b); Pavlov and Berrington (1999); Schunk and Nagy (2009).

<u>The Development of a Theoretical Model for suprathermal electron transport with initial focus on experiments at Arecibo Observatory.</u>

Necessary significant advances have been made to implement theoretical modeling of the plasma line kT_p spectrum as one key future diagnostic (Carlson and Jensen, 2014). One can calculate photoelectron or hypothesize an HF accelerated electron production rate versus energy and altitude, allow for the transport of the photoelectrons or suprathermal electrons, and use these inputs to arrive at the theoretical kT_p spectrum. Also, as noted above, we will seek to compare the experimental kT_p spectrum with one calculated from the observed T_e profile. In contrast to the Mantas [1975a] photoelectron production model, the simulated HF accelerated suprathermal electrons are scaled by a multiplier to a factor times the photoelectron flux in the 20-30 eV range for reference of HF vs. solar produced fluxes. A reconstituted and updated Mantas model [Mantas et al., 1975a,b, 1978] is also used for electron transport and to convert the photoelectron fluxes into kT_p versus E□. Dr. George Mantas provided support in answering

questions concerning his original Fortran code, and, as needed, helped clarify his technique for calculating the transport of photoelectrons, the integration of the electron flux across angular distribution and energy, and the conversion of these parameters into $kT_p(E\square)$. The thermalization of the electrons (e.g. electron/ion/neutral heating/cooling rates, heat conduction, etc.) is also modeled using an updated module in the Mantas program.

The modeling algorithm developed in Year 2 consists of seven modules that are described below.

Module 1. Organizes and converts to uniform units, photo-absorption and photo-ionization cross-sections from various sources to be used in calculation of primary photoelectron (pe) energy flux.

Input: EVE satellite EUV spectrum, photoionization potentials for O, N2, O2

Output: Wavelength and flux intensities, photon flux (photon cm^{-2} s^{-1}); photoabsorption cross-section (cm^{-2}), photoinization cross-section (cm^{-2}), branching ratios (L 1-7), total branching ratio, ionization yield.

Module 2. Computes primary pe energy spectrum and ion production rates. This program module makes use of the output from module 1 along with the following input.

Input: Neutral temperature at 120 km and exospheric temperature (A profile shape parameter is used to insure that the calculated $T_n(h)$ and its altitude gradient are both smooth and continuous); solar zenith angle; wavelength independent scaling factor for EUV flux; atomic weights, number density of neutrals at 120 km, altitude grid points (km) at constant mass spacing.

Output: Thermospheric profiles with smooth derivatives; EUV weighted optical depths; primary pe spectrum (pe cm-3 s-1 eV-1); total electron production rate (electrons cm-3 s-1); total pe kinetic energy (eV- cm-3 s-1 in 1 eV intervals); other relevant pe production rate properties.

Module 3. Computes the steady state pe fluxes (cm-2 s-1 eV-1 str-1). It calculates flux up and fluxes down. It takes the output of Module 2, plus the input below.

Input: Primary pe production rate.

Output: Steady state pe flux into unit hemisphere up and down.

Module 4. Computes the steady state pe fluxes. It takes the output of Module 3 and adds the conjugate pe fluxes when sunlit.

Input: Angular distribution of primary pe source.

Output: Excitation and ionization and calculation of mean free paths and to add conjugate pe flux for the net composite steady state flux (cm-2 s-1 eV-1 str-1), flux up and flux down. Modules 5-7 transform the physical pe parameters in Module 4 into quantities measurable with the AO ISR, in particular, plasma line intensities.

Module 5. Transforms the pe flux distribution to a spherical coordinate system rotated G degrees about the X-axis to be used in plasma line kT_p calculations.

Input: Geometry of radar and local geomagnetic field specifications.

Output: Integration of transformed flux over the azimuthal and polar angles to derive transformed flux.

Module 6. Calculates the 1-D pe density distribution along the radar wave propagation vector to be used in calculating plasma wave temperatures. It uses the output from Module 5 together with the following inputs.

Input: Radar wavelength and beam direction relative to the specified geomagnetic field geometry.

Output: 1-D pe density distribution.

Module 7. Calculates plasma wave temperatures $kT_p(E\square)$ from calculated pe fluxes and

interpolates at requested altitudes and energies (double precision). Input is output from Module 6 plus the following input.

Input: Geomagnetic field specification to calculate electron gyro frequencies, electron density and temperature profiles.

Output: Calculates from YP theory the contribution of thermal electrons, including Landau damping, to plasma line enhancement equation (s cm-4), for up going and down going pe. The ensemble of programs now can trace suprathermal electron transport from HF produced electrons of ~ 1-100 eV as well as primary pe production, steady state pe fluxes, and derive plasma line measurable quantities.

Further new "Module 8" for HF accelerated electron flux energy tracking:
Penetration altitude: In later figures we show the output of the updated Mantas program suite, when we replace the solar produced photoelectron flux at 254 km by a significantly more energy-flat flux representative of an HF accelerated electron flux, as calculated by the methods of Gurevich, A.V., H.C. Carlson, Yu V. Medvedev and K.P. Zybin (2004).

4. Progress on transport

4.a Synopsis: We discovered important changes the community must adopt for its enhanced efforts to test HF accelerated electron energy spectra using the most commonly available means- optical emission line intensities. We applied models of electron transport and impact excitation, to demonstrate theoretically that one of the most commonly used lines (557.7 nm) used for purposes of estimation the spectra of HF accelerated electrons, must be corrected for flux degradation due to energy losses to the ambient electron gas. We furthermore also experimentally verified this. The correction can be half an order of magnitude, and is thus a major one. We also demonstrated a significantly improved observational mode for the upcoming Arecibo Observatory experiments testing production mechanisms and efficiencies. We have reported these discoveries in an Invited Review, August 2014 at the International COPSAR meeting.

4b Rationale: Confirmation (Blagoveshchenskaya et al. 2009; Pedersen et al., 2009, 2010) of the prediction (Carlson 1987, 1993) of production of significant ionization by high power HF radio waves has spurred further work on estimating the energy spectrum (e.g. Gurevich et al, 2004) of HF accelerated electron fluxes. Because incoherent scatter radars, rockets, and satellites are rarely available, estimates of spectra from sets of optical emission lines has drawn increasing attention (e.g. Gustavsson and Eliasson et al 2008, Hysell et al, 2014). This has led us to apply modeling of impact emissions and electron transport to test our understanding. We also examined a unique set of unpublished data we collected at Arecibo during our most recent past HF heating experiment. The experiment leading to these results was designed to provide an independent confirmation of the presence of HF accelerated electrons to energies above 10 eV, i.e. approaching ionization potential, at the mid to low latitude location of Arecibo (18.3° geographic north, L value ~1.5). [Note it has since been theoretically predicted (Gurevich et al. 2002) and experimentally confirmed at all high latitude HF facilities (Pedersen and Carlson 2001; Kosch et al., 2000; Gurevich et al. 2001, 2002, 2005), that there is a significant difference between high vs. lower latitude high power HF effects, due to prediction/confirmation of what has come to be known and embraced as the magnetic zenith effect (see review by e.g. Gurevich et al. 2005). Effects of high power HF transmission at high latitudes can also be significantly

amplified by HF operation at multiples of the electron gyro frequency (Djuth et al. 2005; Blagoveshchenskaya et al. 2009; Pedersen et al., 2010, etc.), which currently are not accessible

The April 1988 optical observations we present here were gathered at 630.0 nm, 557.7 nm and 777.4 nm over the Arecibo Observatory. These have electron impact excitation thresholds respectively of 1.96, 4.19, and 10.74 eV. There has been some confusion in the literature as to "whether the 630 nm HF enhancements are due to thermal or supra-thermal electrons." As a general answer, they can be either or both, depending on the electron density profile (Carlson, 1996). To get thermal excitation of 630 nm emissions requires an electron gas temperature above ~2700 K. For a given HF heating rate, thermal balance leads to an electron temperature determined by the cooling rate of the electron gas. This in turn is dependent on the number of electrons times the number of ions, to which they loose energy in collisions; the electron gas cooling rate depends on the square of the electron density. (See e.g. Mantas et al. 1981 for a detailed discussion of electron gas thermal balance, and the key role of thermal conductivity, within a context directly relevant to this discussion.) If the electron density is near 10^6 cm^{-3} at the height of HF reflection, the F region electron gas is very tightly coupled by to the ion gas, by electron-ion collisions, and its temperature remains close to that of the ions, too low for 630 nm thermal excitation. If the electron density is near 10^5 cm^{-3} at the height of HF reflection, the electron gas cooling-rate is 100 times lower: The electron gas is, in effect, thermally insulated from the local (ion) heat sink, and its temperature can rise very significantly above that of the ions, and be a good candidate to thermally excite 630 nm. For example, at HAARP heating at ~3 MHz away from any resonances will give large T_e enhancements, at Arecibo heating at high HF frequencies will not.

The data we present were collected at the Arecibo Observatory on April 20, 1988, between 02:00 - 03:00 AST (Atlantic Standard Time or local time). The heater was cycled on/off to permit subtraction of background intensities based on the off vs. on cycle. The HF transmitter was on for 2 minutes of each four-minute cycle and off for the other two, operating at 5.1 MHz with 100 KW from each of the four HF transmitter sub-units, into the rectangular dipole field north of the Arecibo Observatory. We have no reason to anticipate measurable thermal excitation. The data in Figures [3 Left, 4a, 5, and 6 Left] are from the second minute on in the four minute cycle 02:24-02:28 AST. Although the natural relaxation time for the O(^{1}D) state is near two minutes, quenching makes a 30-50 s time constant typical for Arecibo HF heating experiments. We used an S-20 extended-red photocathode to feed our ASIP II.

Key is to use an all sky imaging photometer (ASIP). We found that within a single image, the HF electron-impact component of airglow stood out against the background airglow with sufficient clarity that identification was most readily found from subtracting the surrounding 2-D flat field background intensity relative to the intensity enhanced within the clearly defined HF enhanced region. In Figure 5, this can be seen by looking at the intensity contours within the ASIP image. Figure 5 is a reproduction of the original raw data with no processing other than four progressively higher degrees of smoothing over adjacent pixels in the raw image. One purpose of this was first to experimentally verify that there was no "Magnetic Zenith effect" at the Arecibo latitude, as theoretically expected at this low latitude, in contrast to such effects now known at high latitudes. The second purpose was to test how much smoothing would be needed to get good noise statistics on the HF electron

impact excited component of the image, to separate it from the background. So doing within an individual image eliminates problems of varying intensity from one time to the next, a significant improvement reducing noise or bias.

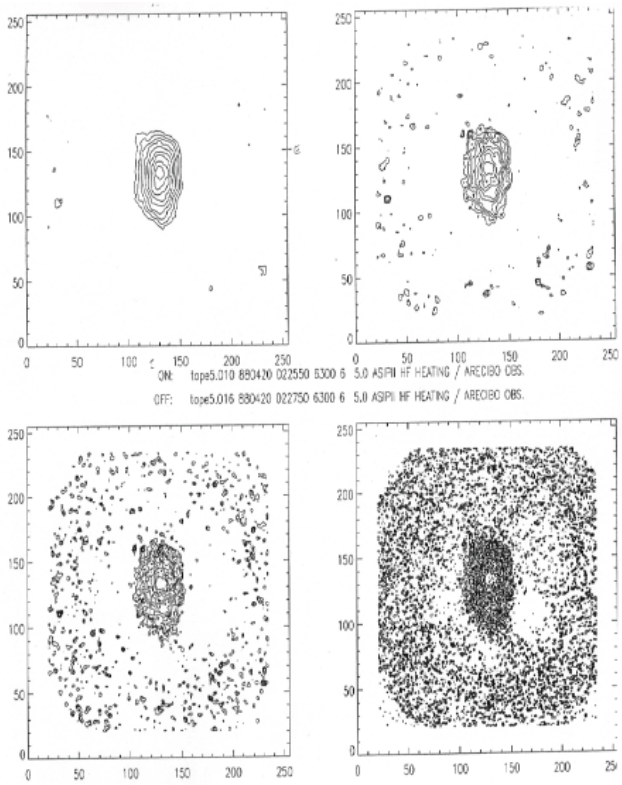

Figure. 5 Original data Arecibo April 20, 1988, for 630.0 nm emission and surrounding background, in single frame image, with no data processing beyond increasing degrees of smoothing of adjacent pixels, to reduce noise fluctuations in image. Clear contours stand out well against background with no further subtraction

We then repeated this step for the 557.7 nm and 777.4 nm images, to get the clearly defined contours of airglow enhancement, within Figure 3-left. Figure 3-left shows Arecibo observations on April 20, 1988, 15 s integrations, in projection of HF electron excited optical emission contours (derived as in Figure 5) for 630.0 nm (red), 557.7 nm (green) and 777.4 nm (violet), horizontally aligned in the magnetic meridian plane, then moved vertically along the magnetic field line over Arecibo Observatory. The vertical scale is about half a neutral oxygen scale height (tens of km)

For the merged Figure 3-left, we needed two further steps:

First, the contours were so well defined, that we could align the contours for each emission line (630.0, 557.7, 777.4 nm) on each other closely enough to define a horizontal (latitude/longitude) displacement of the contours relative to one another. Note that the center peak-intensity-contour in each case aligns well when all lower intensity level contours match best, so all emission contours are consistent with the expectation of excitation electron trajectories being largely confined to move along the magnetic field. Reassuringly we found the center of each set of contours was in the common plane of the magnetic declination.

Second, this conforms to the physical expectation that all emissions should be centered on a common magnetic field line, so the only unknown is reduced to the altitude of the center of

gravity of the emission volume. Therefore, we drew a line with the dip angle of the Arecibo magnetic field line at the time these data were taken (note this is a moving target model for which that can be tracked on the web). With the only remaining unknown as the altitude of the center of gravity of the emission contours, within this one-degree of freedom we slid the contours up or down the magnetic field line to center the contours about that line. Putting the field line through the center of one emission line then defined the altitude of the other two. As expected the 630.0 emissions is at the highest altitude (near the source region). We then find the 557.7 emissions closely below it, and the 777.4 emissions lowest in altitude. This is consistent with one's first-reaction intuition in that harder particles penetrate more deeply into the atmosphere than softer particles. We shall discuss this further in the modeling section.

We plot both this Arecibo data and the HAARP data on a common diagram, Figure 3, to help us remember to "keep the end in mind from the beginning." Our goal is to use optical emissions as a tool to help understand the spectrum of the HF accelerated electrons, with particular emphasis on relevance to production of significant ionization. We have long known some ionization is produced (e.g. Carlson et al. 1982), the issue here is whether significant ionization is produced, relative to that by the sun (Pedersen et al., 2009, 2010). Figure 3-right shows data from HAARP, of 557.7 nm volume emission rates, on altitude vs. horizontal distance scale. It shows only 557.7 nm emission intensity, so the color scale represents different degrees of 557.7 nm intensity. This is from a publication (Pedersen et al. 2010) which also shows ionization production peaks nominally collocated with the 557.7 nm emission peaks, so Figure 2b color contours of most significant electron impact emission excitation are nominally indicative of regions of most significant ionization production. In this sense on Figure 3-left, the
777.4 nm emission (violet), is at energies (>10.7 eV) closest to the ionization potential for atomic oxygen (13.6 eV). We can now move forward to the modeling component of the study enabling our conclusions.

4c Electron transport and impact: The initial plasma line work estimating HF suprathermal electron fluxes, used a software package described in Carlson et al. (1982 and references therein) and from their Figure 6, reproduced here as our figure 6. Prof. Mantas kindly worked with us recently at USU to enable us last year to revitalize this software, re-compiling to run on today's machines. For consistent baselines, changing only one thing at a time, we have run these programs with the same cross- sections/rates as in 1982, so comparisons can initially remain in a common frame or reference. Comparison of our data herein, with output from these models below, is quite instructive beyond this data set alone. It offers value for optimizing future data collection as well as interpretation of past and future data.

Model runs in Figures 6, 7, 8 all use an MSIS thermosphere model input, with very minor smoothing to keep both neutral density and its altitude derivative smooth for purposes of computer program stability. The actual measured electron density profile was included for their Figure 6 (Carlson et al. 1982), here in the absence of a measured electron density profile we omitted that input to the program for Figures 7 and 8. Recall we are comparing profiles of optical emission from the thermosphere, not electron densities or plasma lines in the ionosphere.

As done in Carlson et al. (1982), we start with injection of a flat spectrum of electrons within a single thin altitude slab, to represent a thin slab within which HF excited plasma instability processes would produce a thin electron flux source region (as detailed in e.g. Gurevich 2007 and references cited therein). Figure 7 shows the results for a thin altitude source slab of HF accelerated electrons at three altitudes, one at which the thermosphere is: very optically thin (982 km) far right hand side, intermediate (505 m) center, and optically thick (254 km) left hand side of figure. The optically thin case is similar to the model first published by Haslett and Megill (1974), based on their observations at the Platteville heater near Boulder CO, and which is also representative of Arecibo conditions well before "midnight collapse". The up-going flux largely escapes to the conjugate hemisphere and the down-going flux barely penetrates to 250 km on this scale. For the HF electron source slab in the optically thick region, most of the flux is absorbed within a neutral scale height on either side of the source region. This latter case is representative of Arecibo conditions with midnight collapse near full descent. The intermediate slab location is indeed intermediate. The only difference between the upper vs. lower triple of plots in this Figure 8 is a sufficiently different flux scale, to readily show a fifty-fold range of flux intensities. "Midnight collapse" is a name given to a regular feature of lower mid-latitude ionospheric nighttime behavior, where the ionosphere held up at very high altitudes by neutral winds, falls by ~50-100 km or more when the neutral winds abate often shortly after midnight (see e.g. Gong et al. 2012).

Figure 8 shows results from calculations with the same updated model as for Figure 7, but now in the form of altitude profiles of steady state flux binned for optical emission of 557.7 nm, 777.4 nm, and for electron impact ionization, all for atomic oxygen (thresholds respectively of ~4.2, 10.7, 13.6 eV). Figure 3 of Carlson et al 1982, had been for 2 eV bins of flux flat from 0-20 eV, to establish electron acceleration up to at least 20 eV, above thermosphere ionization thresholds. By now theory has advanced to make the more relevant question where between 1-100 eV does the electron spectrum essentially cut off, so in Figure 8 we work in 10 eV bins of flux flat from 1-100 eV. One finds the essential information for insight is well captured by the 70-80 eV examples, where we therefore choose to stop showing examples.

Perhaps the most straightforward set of plots to follow is the optically thin case in Figure 8A, with the single-altitude electron-flux-source at 982 km. First, look only at 10 eV wide bins. For 1-10 eV, only 557.7 nm shows any emission, because the other two thresholds are >10 eV. Ten eV bins of 20-30 eV or higher all follow a common well defined pattern where more energetic particles penetrate deeper (including that profiles for production of O^+ penetrate more deeply/ generate higher yields at each height than 777.4 nm, and 777.4 nm likewise relative to 557.7 nm). The 10-20 eV bin is mixed because of secondary/cascading-energy electron fluxes. Next examine the integral plots of 1-20, 1-40, 1-60, and 1-80 eV plots; they have a clearly different pattern in that the 557.7 nm curve (in sharp contrast) always shows 557.7 nm peaking below to lower energies. We shall say more about this in the discussion section. Figure 8B is the same as Figure 8A, except for the optically thick case (electron source flux flat 1-100 eV, in a single altitude slab at 254 km). These optically thick

cases exhibit the very same main qualitative and semi-quantitative features. For all 10 eV bins 20-30 and above, the O^+ production profile always penetrates more deeply than 777.4 nm, the 777.4 nm profile always penetrates more deeply than the 557.7 nm profile. The profiles for the integrals spanning 1-20, 1-30, 1-40, …, 1- 80 eV the 557.7 and 777.4 penetration depth reverses, and 557.7 nm profiles are all lower in altitude, not higher, than for the only 10 eV-wide bin profiles. The same explanation applies, the secondary electrons cascading down to below 20 eV energy add up to strongly enhance the <20 eV part of the profile.

The intermediate case between Figures 8A and 8B (not shown here for brevity of presentation) showed the same pattern for that case of an electron source region in a single altitude slab intermediate between an optically thin and thick case. Also common to optically thin through thick cases, the emission profiles for 10-20 eV are at virtually the same height for 777.4 and 557.7 nm, so it is only the contribution for electron fluxes or energy < 10 eV that accounts for this 777.4 vs. 557.7 penetration height reversal. We will revisit this as well in the Discussion section.

Note that Figure 7 here is for the integral flux 1-100 eV only. Similar plots were also done for a series of ten 10 eV wide bins, to see how a single 10 eV energy bin would cascade and fill in lower energies with its secondary, tertiary, etc. electrons. Once the 10 eV bin reached 40-50 eV and above, there was an ~20 eV discontinuous jump (e.g. a 10 eV wide bin from 50-60 eV, would yield negligible 40-50 eV secondary electrons, but fill in below) (20 eV wide bins had no such gaps). This ties to the idea that for the F region one needs an additional 20 eV to get another ionization. (In the E Region it is ~35 eV per ionization pair (Rees and Roble 1986).)

Now we are ready to compare the observed optical emission altitude to those from our model calculations to see what we learn.

4d Discussion: Recall the motivation for this research area is to see what we can learn about the HF accelerated suprathermal electron energy spectrum. At a more general level, the goal is to work backwards from measurements of optical emissions at several different wavelengths, to estimate the energy spectrum of electrons present. This is somewhat analogous to the problem of using optical data of the nature to make estimates of auroral particle fluxes (e.g. Strickland et al. 1983), except in their auroral case they could narrow assumptions about the electron spectrum to two models– a Maxwellian and a Gaussian distribution. In this HF field of study we are still early in developing the theory, and need experimental guidance to help its further development (e.g. Gurevich 2007). Gustavsson and Eliasson (2008) used optical emissions to set parameters in a physics based model. Hysell et al. (2014) employed a non-parametric based inversion approach. Sergienko et al. (2012) used a Monte Carlos model for electron transport. These papers give some context for our work here in terms both seeking more realism of conversion of optical observations to suprathermal electron fluxes, and remaining mindful of mutual dependence/independence of assumptions about theory. We will address a missing term in the equation and observations to estimate its magnitude.

To put our 777.4 nm observations in current observational context, by now the compliment of optical instruments that have been fielded span: red-line emission at 630 nm associated with the radiative relaxation of the $O(^1D)$ state with excitation threshold of 1.96 eV; green-line emission at 557.7 nm associated with the radiative relaxation of the $O(^1S)$ state with excitation threshold of 4.19 eV, 777.4 nm from the radiative deactivation of the 3p5P state of atomic

oxygen with an excitation threshold of 10.74 eV, 844.6 nm in the F region mainly from electron impact excitation of atomic oxygen in the 3p3P state, with excitation threshold is 10.99 eV, and the blue-line emission at 427.8 nm associated with electron impact ionization of molecular neutral nitrogen and the subsequent excitation of the B2 state, with excitation threshold of this state is 18.75 eV. For production of ionization in the F2 region dominated by atomic oxygen, the ionization potential is 13.62 eV. (Note: Only one relevant observation is known to date during heating experiments for this (Mutiso et al. 2008), namely O^+ 732–733 nm emission, found consistent with electron impact ionization. The importance of collisional quenching of $O(^1D)$ (negligible for the $O(^1S)$ state or other prompt emissions in the F region) are well known, and other complications have been long discussed (Rees and Roble 1975); related work still continues (Kalogerakis et al. 2009).) Our focus here will be use of the compliment of wavelengths as they relate to diagnosing suprathermal electron spectra.

In comparing our data with the model profiles, the most striking thing is the discrepancy in the height of the observed vs. modeled 777.4 vs. 557.7 nm emission profile. They are opposite to that from the energy integral flux. The altitude of the observed 777.4 nm emission is based on simple geometry, it is farther down the magnetic field line from the electron source region. The model profiles as implemented do have one issue, as explicitly noted in section 3, they do not include suprathermal electron flux losses to ambient background electrons. We did find that if we left out suprathermal electron fluxes below 20 eV, 777.4 nm emission would be from more deeply penetrating electrons and the profile would be below that for 557.7 nm, as the observations show. Since the emission profiles for 10-20 eV are essentially the same, it is really only the electrons below 10 eV that lead to 557.7 nm being the lowest altitude for all emission profiles. At these low energies (<10 eV) we still have a competition between losses to the ambient electron gas (omitted), and $O(^1D)$, $O(^1S)$ and vibrational excitation of N_2 all included. Qualitatively we know energy loss of suprathermal electron energy to ambient electrons is preferentially below 10 eV, but what can we say quantitatively?

Abreu and Carlson (1977) have published the impact of photoelectron energy losses to ambient electrons, as experienced at Arecibo (the same energy range as here), and compared their observed loss to that calculated from theory (Schunk and Hays 1971). We reproduce their Figure 8 (Abreu and Carlson 1977), as our Figure 9 here. We see their agreement between observation and theory was remarkable. Most importantly for our work here, is the impact on 557.7 nm emission of adding that loss of suprathermal electron flux below 10 eV. The impact: reduce the 557.7 nm emission on the bottom side by a factor exceeding half an order of magnitude; reduce the calculated bottom-side 557.7 nm emission to less than that calculated for 777.4; and restore 777.4 nm emission to being at a lower altitude than 557.7 nm. It leads to a much-reduced role of secondary electrons for impact excitation of bottom-side 557.7 nm profiles.

For analysis of optical data, if we want to look at individual emission lines we have lost little, they are each instructive in their own way. If we want to combine 557.7 nm emissions with higher energy threshold emissions to derive a suprathermal electron spectra, we now have to work harder than previously generally realized. Losses of secondary electron impact excitation of bottom side 557.7 nm emissions must be factored into analysis. Figure 10 illustrates ample cross-sections and a theoretical spectral prediction for the conditions anticipated at Arecibo.

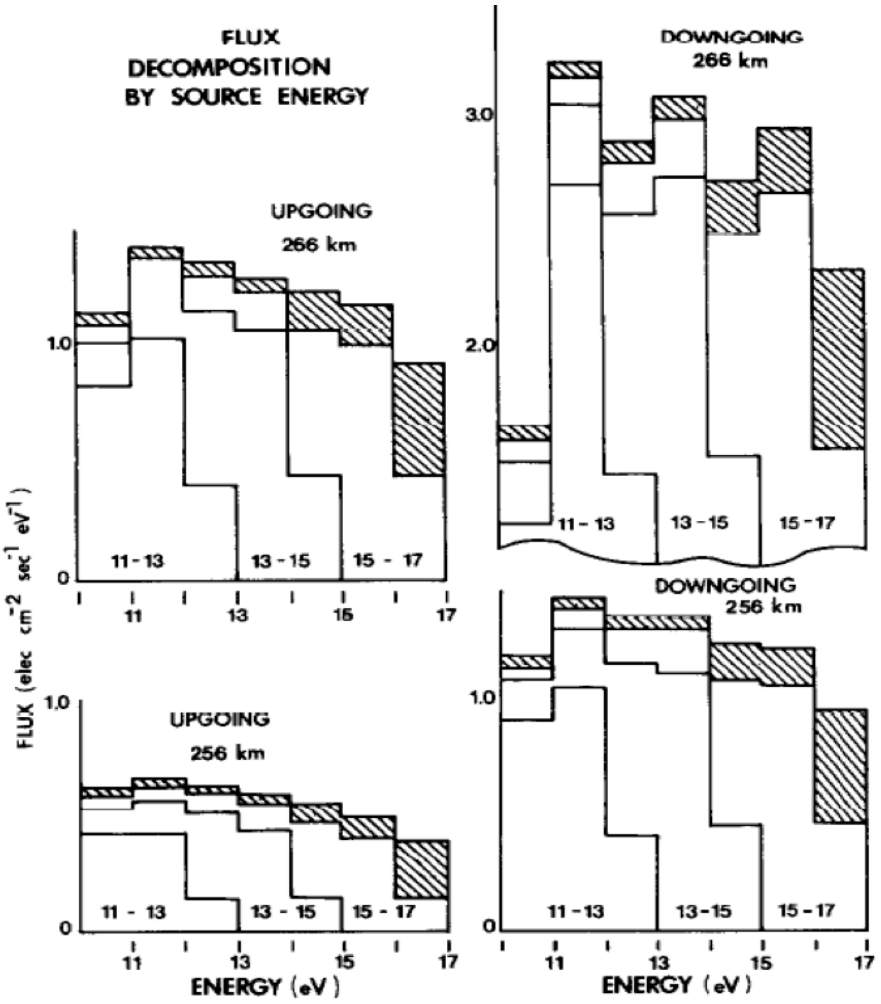

Figure 6: Relative fluxes of up-going and down-going suprathermal electrons at several altitudes in the observation region were derived from a uniform production rate from zero to 20 eV electrons, all originating at 275 km. This figure shows their decomposition by energy of the up-going and down-going suprathermal electron fluxes at 256 and 266 km. The calculations partition electrons into 2 eV segments of the spectrum at 275 km, and was traced to other energy ranges at lower or higher altitudes. The right-hand figure shows the downward flux at the two altitudes. The left-hand figure shows the upward flux obtained from electrons backscattered at the indicated and lower altitudes (Carlson 1982)

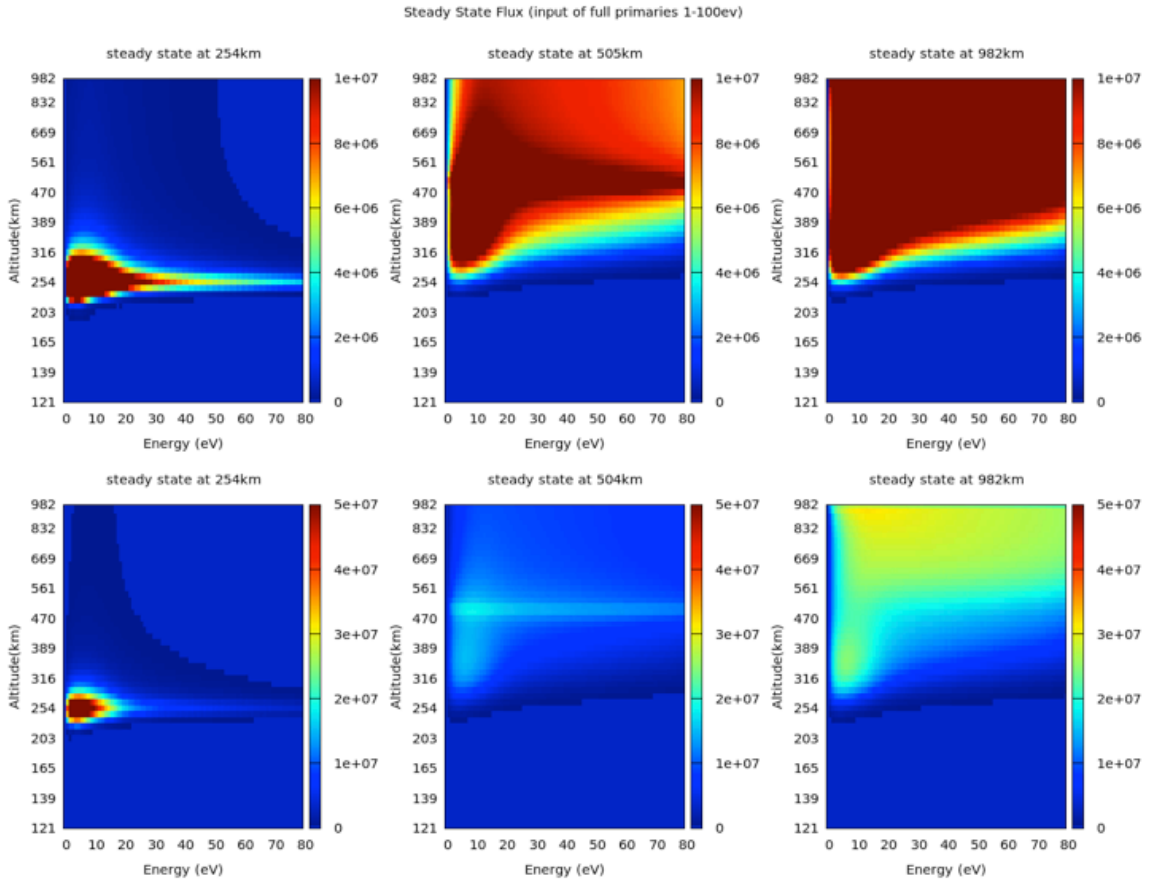

Figure 7: Shows the results for a single thin altitude source slab of HF accelerated electrons at three altitudes, one at which the thermosphere is: very optically thin (982 km) far right hand side, intermediate (505 km) center, one at a depth at which the thermosphere is optically thick (254 km) left hand side of figure, and one intermediate (505 km) in the central column of the figure. The only difference between the top and bottom row is the flux scale, to visualize a dynamic range of a factor of 50 in suprathermal flux. This shows penetration depth of composite electron flux including all primary and secondary electrons

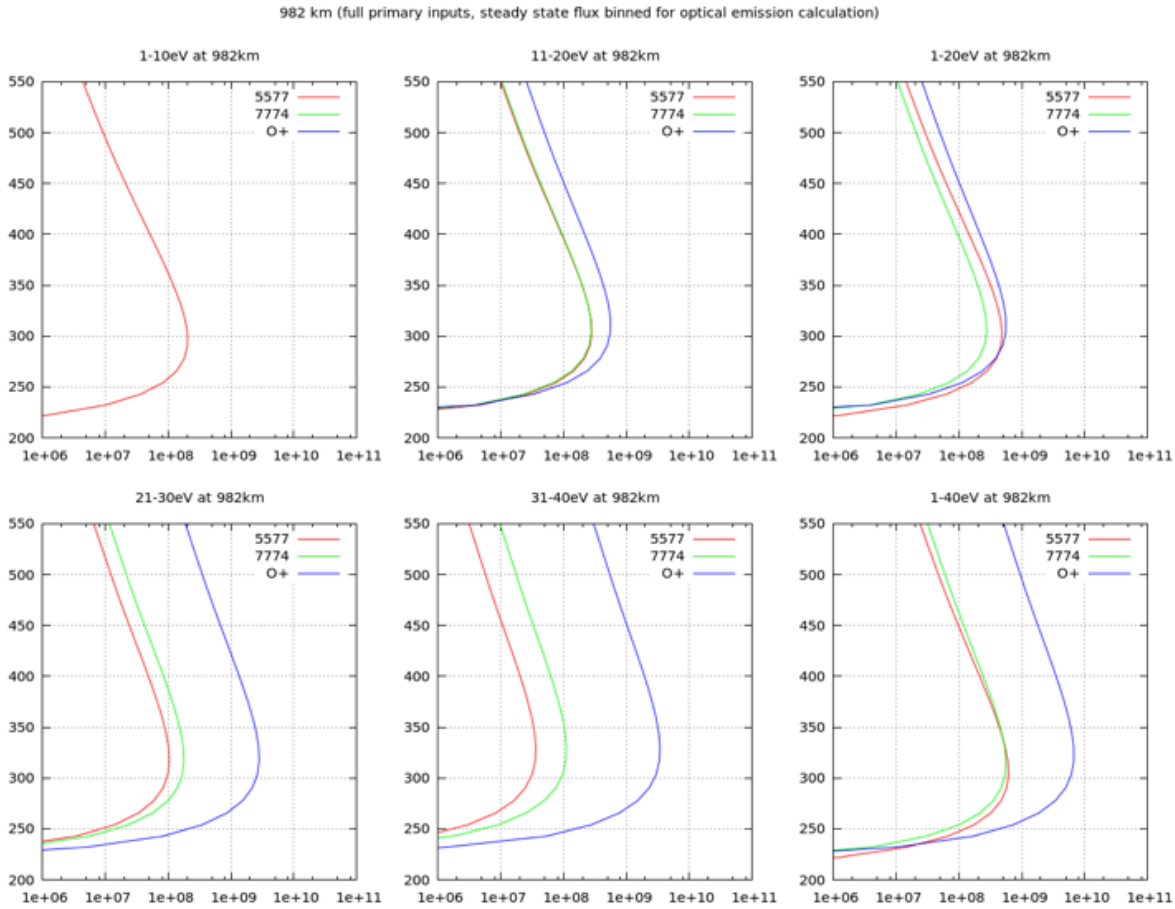

Figure 8a: Shows results from calculations with the same model as for Figure 4, but in the form of altitude profiles of steady state flux binned for optical emission of 557.7 nm, 777.4 nm, and for electron impact ionization, all for atomic oxygen (thresholds respectively of ~4.2, 10.7, 13.6 eV). While Figure 7 was for the sum of all primary and secondary electrons, Figure 8 inserts the primaries in 10 eV wide bins, one at a time (still all equal and flux flat between 1-100 eV), and shows the sum of these primary electrons plus all secondary electrons that 10 eV wide bin produced. Figure 8A is for the optically thin case, electrons injected in a thin slab at 982 km.

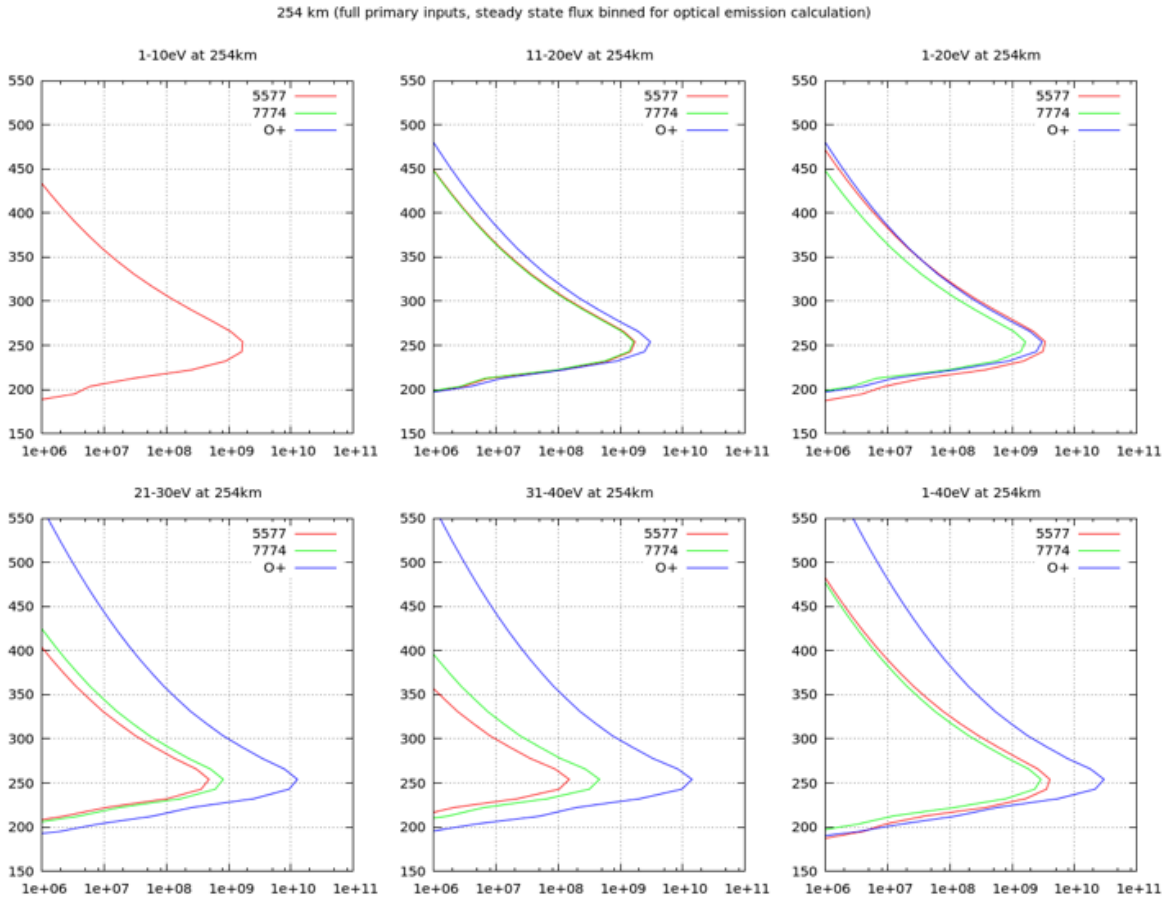

Figure 8b: Same as figure 8a except for the optically think case , electrons injected in a thin slab at the altitude of 254 km.

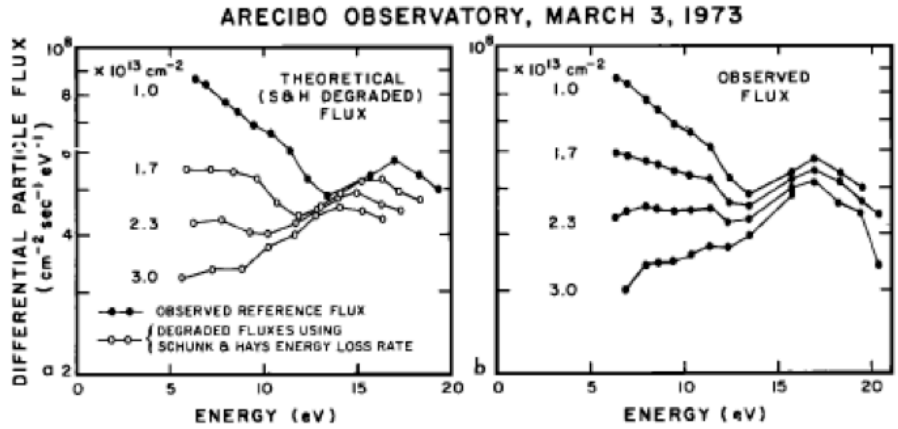

Figure 9: (a) Differential particle fluxes obtained by degrading the experimental spectrum shown in Abreu and Carlson (1977) Figures 8a and 8b at 1.0 x 10^{13} cm^{-2} using the Schunk and Hays (1971) energy loss expression; (b) The observed differential particle fluxes for matched conditions.

4e The findings of Carlson and Jensen (2014) established:

First, we have observed HF electron impact excited optical emissions at Arecibo from 630.0 nm, 557.7 nm, and 777.4 nm wavelengths. In and of itself, the 777.4 emission is unequivocal proof that at Arecibo we had HF accelerated electron fluxes accelerated to energies >11 eV. Within the context of their persistence and the persistence of plasma line enhancements observed previously (Carlson et al. 1982), plus the experimental and theoretical evidence for spectral flatness across 10-20 eV (Carlson et al. 1982; Gurevich et al. 2000), we conclude that observation of 777.4 nm (Carlson and Jensen, 2014) and 844.6 nm (Hysell et al. 2014) emissions (respectively 10.74, 10.99 eV) are a good surrogate for presence of HF electron fluxes in the ionizing range (13-19 eV).

Second, even this alone demonstrates that observations of each of many individual wavelengths have been and continue to be of value to help guide theory of plasma physics and potential applications as e.g. production of artificial ionospheres.

Third, regarding spectra, to construct or guide theory to improved prediction of HF accelerated *energy spectra based on energy integrals* constrained by optical observations, further effort offers good value (e.g. Gurevich 2007 and many references therein). Gustavsson et al. (2005) used optical emissions to set parameters in a physics based model, but then returned in Gustavsson and Eliasson (2008) to notably improve realism of the findings by adding altitude dependencies of fluxes. Hysell et al (2014) introduced and applied a method to estimate the suprathermal electron population versus altitude and energy, during an F region HF ionospheric modification experiment, on the basis of observed emissions and an inversion method based on a variation of the classic Backus and Gilbert approach, including utilization of Green's functions to reduce the dimensionality of the problem. The nonparametric method was in contrast to the Gustavsson and Eliasson (2008) approach using airglow emissions to set the parameters of a physics-based electron acceleration model. They do a thorough listing of the competing cross-sections, including N_2 vibrational excitation essential to the composite electron impact cross-sections in the 1.5-5 eV range (Itikawa 2006). The Hysell et al. (2014) work was motivated by not overly constricting derived spectra to input assumptions about a spectral shape from a theory still in development. Sergienko et al. (2012) have explored improvement in electron transport with a Monte Carlo method. Hysell et al. (2012) has likewise explored applying spectroscopy to estimate electron energy spectra and Eliasson et al. (2012) have done numerical modeling of artificial ionization layers at HAARP. Gurevich et al. (2004) have started from a theoretical derivation of HF accelerated electron fluxes noting optical emissions to which they should give rise. Work remains active to close this loop.

This work was similarly motivated by seeking understanding of limits and opportunities for more fruitful analysis of past and future data, and more robust was for future data collection, with the specific goals of combining multiple wavelength optical observations for improved realism of constraints on derived electron energy spectra.

Issues with 630.0 nm are well discussed in the literature (Rees and Roble 1975; Kalogerakis et al. 2009). In assessing the importance of N_2 particularly of electron impact excitation of vibrational states (Itikawa 2006), it is important to keep track of the altitude dependence of number density of atomic oxygen vs. molecular nitrogen, the ratio of which increase approximately an order of magnitude when going down in altitude from ~300 to ~150 km.

We document the importance of suprathermal electron loss to the ambient electron density in the F region. For our representative observations introduced here, we find that inclusion or

omission of this loss term in the calculation makes the difference between the 557.7 nm emissions being above or below the 777.4 nm emission peaks. To make a more useful statement applicable at a general level, we highlight experiment and theory in agreement that an electron content of ~$2x10^{13}$ cm^{-2} degrades the component of a flux of suprathermal electrons of energy < ~10 eV, by about half an order of magnitude. This pertains to high nighttime electron densities, which are particularly attractive for HF heating experiments looking to work at higher HF frequencies for maximum HF power on target and electron acceleration.

For experimental work, it is thus important to measure/estimate electron density profiles if one wishes to use 630.0 and/or 557.7 nm data in conjunction with higher energy threshold emissions (e.g. 777.4, 844.6, 427.8) to construct suprathermal electron energy spectra.

Specific techniques for design of experiments, data collection, and data reduction are highlighted here, both for general collection and including specific focus on Arecibo, where resumption of heating experiments is imminent, making these specific findings timely.

It is worth noting that from calculations tracking the cascade of energy from above 40 eV, it appears that the number of eV per ion pair produced is closer to 25 eV per ion pair in the F region than the conventionally quoted nominal rule of thumb of 35 eV/ionization pair (Rees and Roble 1986), which is more associated with E region aurora. This distinction may be of interest more generally for work on planetary atmospheres. In that community, Simon et al. (2011) treat this question in detail for five planetary atmospheres, and Fox et al. (2008) have delved deeper into tracing energy flow and deposition for other atmospheres.

We should point out that here in closing, that by design, the altitude of the source electrons in these calculations was defined as being held fixed, so the program was not intended to track a downward motion of an artificial ionization layer were such motion to occur as at HAARP (Pedersen et al. 2009, 2010). A program to track downward descent of any artificial ionization layer formed, would require full transport tracking of ambient background electrons through the thermosphere, in contrast to just the supra-thermal component discussed here.

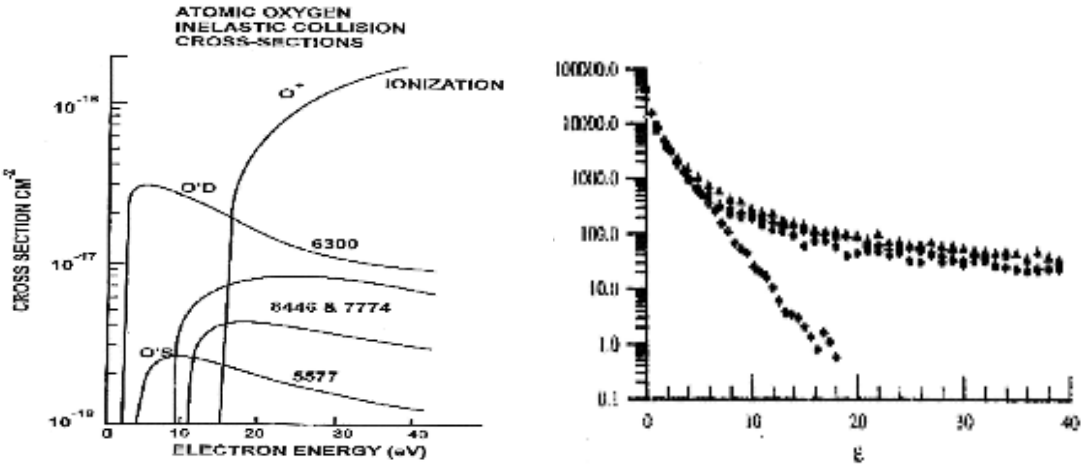

Fig 10: (left) Collision crossections for electron excitation of atomic oxygen emissions. (right) Calculated HF accelerated electrons, from Gurevich, A.V., H.C. Carlson, Yu V. Medvedev and K.P. Zybin (2004), and showing relatively flat spectrum above where it deviates from the background thermal Maxellian electron population distribution.

5. Definitive Test of ionization production at Mid-Latitudes

5.1 Introduction/motivation:

Twenty years ago it was predicted (Carlson, 1987, 1993) that once ground based HF transmitters reached the GW ERP class, the HF power densities they would deliver to ionospheric altitudes should be expected to be able to create an overhead ionosphere of plasma density approaching that from the sun, at least at lower mid latitudes. By now technology has achieved such power densities. Experiments to test the prediction were possible first at high latitudes were accessible first, leading to confirmation of the prediction there (Pedersen et al, 2009, 2010; Blagoveshchenskaya et al. 2009). However, phenomena unique to high latitudes [HF trapping and multiple plasma resonances] were shown to be critical to the causative phenomena, and the general case for "unaided" mid-latitude conditions [where processes favoring such production involve critically different physics] remained untested, until the experiment we report here.

The original Arecibo experiment (Carlson et al, 1982) on which the prediction was based, remained the one and only existing experiment at mid latitudes. Key to the prediction was with what efficiency is it possible to convert fry energy [HF radio waves] into ionization rates. Just before experimental confirmation could be tested, Hurricane George (September 1998) destroyed the Arecibo HF heating facility. It was not before November 2015 that the mid-latitude facility was restored to operation, [including significant experimental upgrades] enabling test for validation.

Critically important different geo-plasma-physics applies at *high latitudes, in contrast to mid-latitudes* which are free of MZ effects and other high-latitude geo-physics associated with HF incidence near parallel to B (Gurevich et al, 2002) at SURA, HAARP and Tromso. At high latitudes, theoretical work (Gurevich, Carlson and Zybin, 2005) and experimental test (Blogoveshchenskaya, Carlson et al, 2009) led to the conclusion that the combined effect of upper hybrid resonance and gyro resonance at the same altitude gives rise to strong electron heating, the excitation of striations, HF ray trapping and extension of HF waves to altitudes where they can excite Langmuir turbulence and fluxes of electron acceleration to energies that produce ionization. The essential physics for realization, is to convert HF electromagnetic (EM) into an ionizing form of energy. This was hypothesized and confirmed to be by acceleration of ambient electrons to of supra-thermal energies via acceleration driven by HF excited plasma instabilities. At high latitudes such as HAARP that physics includes two critical steps: (1) plasma-structuring processes [including trapping of the HF EM energy for nearly complete deposition into the ionospheric plasma], and (2) a resonance matching condition that amplifies efficient plasma-instability conversion of the radio frequency energy into electron acceleration.

At low latitudes such as Arecibo, trapping is not possible, and creation of supra-thermal electrons is by a different class of plasma instabilities. At these latitudes only one pass of the HF wave through the plasma is available to deposit energy into ionization production. Confirmation at high latitude cannot fully equate to at low latitudes. It is essential to test independently in both regimes. The November 2015 experiment at Arecibo let us: test the initial prediction based on the old Arecibo experiment, scale to higher power densities, and in light of current theory test important dependencies on further geophysical processes we have learned should be important.

We will confirm that while high vs. mid latitudes have major differences for the steps leading up to supra-thermal electron production, they as expected share dominant commonalities for the physics of the subsequent steps, in which accelerated electrons must be transported from their acceleration region to where their collisions with neutrals yield ionization. At high altitudes near or above ~250 km, this can be many neutral scale heights; near or below 200 km the production can be nearly local.

5.2 Background

An O-mode HF pump wave couples through striations into electrostatic (upper hybrid UH) waves at the upper hybrid resonance altitude, several km below the HF reflection height of the HF heating wave. UH waves propagate near perpendicular to B, their energy dissipation heating ambient electrons. Via thermal instabilities UH waves can excite artificial field aligned irregularities (AFAIs) through thermal instabilities, which can trap the UH electric field. Non-linear stabilization of the striations (Gurevich et al, 1995), self-focusing of the HF pump wave due to the density depletions within the striations (Gurevich et al, 2001), and excitation of density/temperature gradient driven instabilities (Franz et al 1999), compliment generation mechanisms. Striations are generated near the UH resonance altitude where the heater frequency is :

$$f^2_H = f^2_{UHR} = f^2_p + f^2_{ce}$$

where f_H is the HF heater frequency, f_{UHR} is the UH resonance frequency, f_p is the local plasma frequency, f_{ce} is the electron gyro-frequency [electron-cyclotron frequency].

HF heater frequencies near harmonics of the electron gyro-frequency

$$f_H = nf_{ce} = f_{UH} = (f^2_p + f^2_{ce})^{1/2}$$

have underscored the important consequences of HF heating at electron gyro-frequency harmonics. At high latitudes operation at the third and higher harmonics (n = 3 or greater integer] have suppressed 630.0 nm emissions while Djuth et al (1995) showed strong enhancement of 630.0, 557.7 and 777.4 nm [excitation thresholds of 1.96, 4.19, and 10.74 eV] to prove strong enhancement of ambient electron acceleration. This interlocks with strong enhancements of AFAIs produced with the Plattville CO HF heater at twice the electron gyro-frequency, the motivation for Djuth to propose the HAARP experiment at an electron gyro-frequency multiple of n = 2.

High power ionospheric modification research was introduced in the open literature by Utlaut and Cohen (1971) at Plattville. Findings were based on HF heater induced airglow, spread F and wide band field-aligned ionization structure, and wide-band absorption. Work at the Arecibo Observatory soon added measurements of profiles of plasma temperature heating and electron density redistribution, as well as the

experimental discovery that HF power densities sufficiently great to enhance the bulk electron gas temperature have associated electric fields sufficient to drive instabilities in the space plasma4. Increasing the plasma bulk temperature can vertically redistribute bulk plasma density profiles; instabilities can lead to plasma structuring and also acceleration of a small fraction of the electron population leading to impact excitation of optical emissions in the upper atmosphere. Observations of HF excited 630.0 which can be excited by values of Te <~2700 K plus supra-thermal electrons, and 557.7 nm optical enhancements were common, were evidence of impact excitation by electrons of energy > 4 eV.

Prevailing theory in the 1970s dictated that acceleration of electrons (thermal energy ~0.1-0.2 eV) could not exceed a few eV, far below the threshold for production of ionization. An Arecibo experiment proved that theory to be wrong, observing electrons accelerated to energies sufficient to produce ionization (Carlson et al, 1982), who also therein explained semi-quantitatively that the physics of aeronomy to the earlier plasma physics, adding elastic scattering of accelerated electrons, must lead an electron to experience multiple passes through the electron acceleration region. It thus had to reach much higher energies than theory previously gave, thereby explaining the observation of electrons accelerated to 10s of eV vs. a few eV. (HF excited plasma waves can transfer energy to electrons by the landau damping mechanism, with local acceleration experienced as the electrons cross cavitons, now able to have multiple passes vs. a single pass through the acceleration region. This more complete physics was incorporated into the quantitative theory by Gurevich et al (1985), to enable more realistic modeling.)

Ambient electrons of thermal energy ~0.1 eV are heated to thermal energies a few times this by natural solar driven processes by day, and also three to four times this by deviative absorption of fry energy incident from ground based HF Heating experiments. Electrons in the tail of this distribution are also accelerated to energies ~100 times their thermal energy by plasma instability processes. Electron energies of tens of eV are now accepted as fact, based on observations by radar techniques (25eV by Carlson et al, 1982) and modest extrapolation above energy thresholds for observed optical emissions exceeding order 10 eV (up through 11 eV by Bernhardt et al, 1989, Pedersen et al, 2003, Carlson and Jensen, 2014, Kosch et al, 2000, Djuth et al, 1999, and 19 eV by Gustavsson et al, 2005). The ionization potentials of atomic oxygen O, N2, O2 are respectively 13.62, 15.58, 12.06 eV.

Structuring of plasma density has been theoretically derived in significant rages: 5-10 m, 100-200 m, and 2-5 km. Strongly elongated plasma irregularities (striations) producing field-aligned scattering extending up to ~10 km along Earth's magnetic field **B**, are found ~ 5-10 m across **B**. Groups of striations are found in clusters ~100-200 m across **B**. These are found in zones of striations ~ 2-5 km cross **B**. Remarkably, these were first predicted over a series of papers culminating in this semi-quantitative prediction (Gurevich et al, 1995), followed by a Rocket shot (Kelly et al, 1995) confirming them.

At high latitudes they contribute to what the HF community has come call the magnetic zenith effect and HF trapping [figure 12 upper frame]. At lower mid-latitudes the field aligned irregularities are also observed, but with different consequences including the

absence of HF propagation trapping geometry [figure 11 lower frame]. Also critical is the angle (near parallel or near perpendicular) of the HF electric field **E**, relative to **B,** for HF propagation between the height of reflection and the altitude of matching to the UH frequency (Gurevich 2007). The amount HF power that is perpendicular to B at the upper hybrids resonance at HAARP is ~ 45% if the HAARP ionospheric foF2 could support heating at HF = 8.175 MHz; whereas at AO it is only 1.5% at 8.175 MHz.

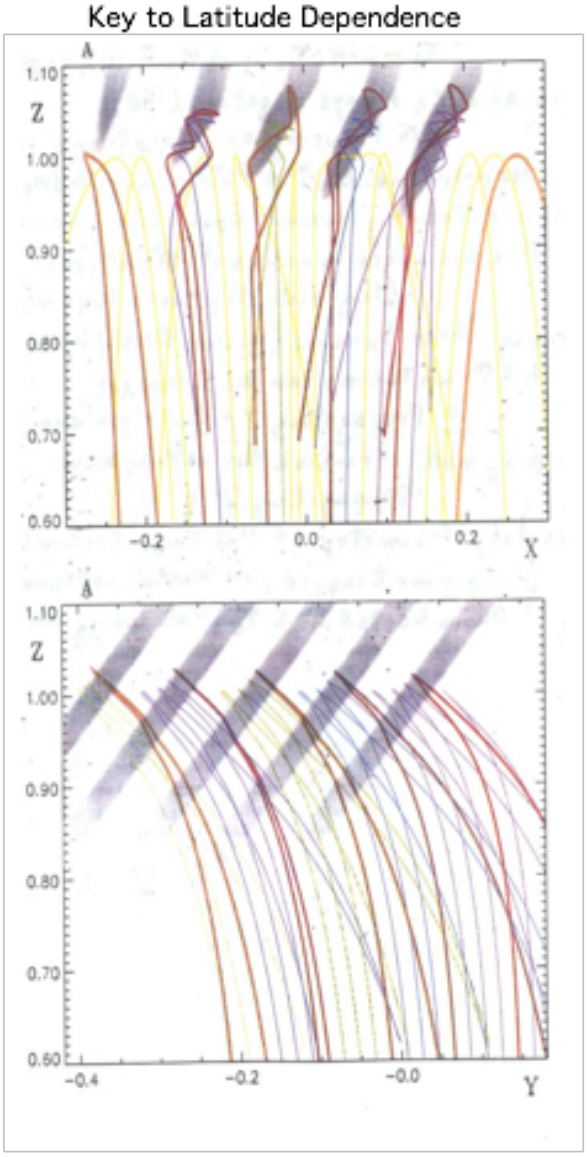

Figure 11: HF fractional trapping. Top pertains to High latitudes [HAARP, EISCAT-Tromso, SURA]. Bottom pertains to midlatitudes [Arecibo] (Gurevich, Carlson, Kelley, Hagfors, Karashtin and Zybin, 1999).

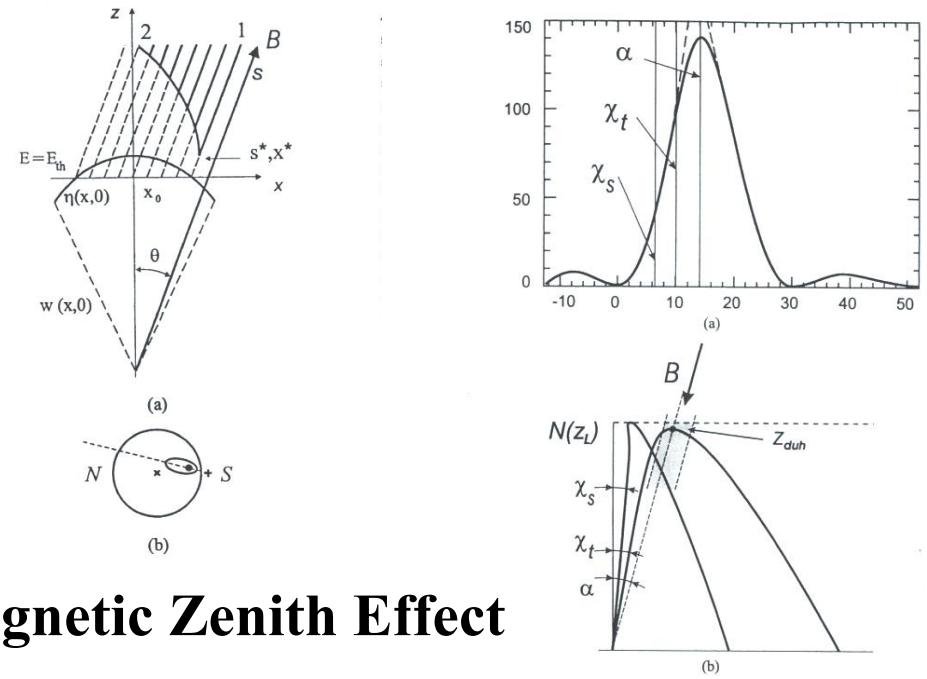

Magnetic Zenith Effect

Important: Sura, EISCAT, HAARP

Left: (Gurevich, Carlson, Zybin, 2001)

Right: From 2 to 3 dimensions (Gurevich, Carlson, Pedersen, Zybin, 2001)

Figure12: A key element of physics underlying the critical difference between high- vs. mid-latitude phenomena is the "magnetic zenith effect".

5.3 Production of plasma by high power HF radio waves:

The one existing quantitative prediction that a significant amount of space plasma (competitive with that produced by the sun) could be produced from the ground (Carlson, 1987, 1993), projected that threshold would be passed once HF radar technology realized GW ERP levels. That quantitative prediction was based on comparison of the HF power density that could be delivered to the F Region space plasma environment relative to that from the sun, which produces our natural ionosphere. From e.g. Rishbeth and Garriott (1969), an overhead sun for average solar conditions (sunspot number ~60) leads to an electron production rate of $\sim 10^3$ cm^{-3} s^{-1} in the ionospheric F region peak, which spread over ~100 km (two atomic oxygen scale heights) gives a column ionization rate of ~1010 ionizations cm^{-2} s^{-1} columnar rate. For ~30eV per ionization by electron impact ionization this represents 3 10^{11} eV cm^{-2} s^{-1} = 4 10^{-8} W cm^{-2}. A GW ERP class HF facility would deliver ~1.3 10^{-7} W cm^{-2} at ~250 km altitude overhead.

A more direct way of expressing this, by making use of the experimental fact the auroral secondary electrons are found to produce one ion per 36 eV of incident particle. Taking 30 eV per ion as more realistic (Carlson and Jensen, 2014) for the HF accelerated

electron spectrum, would lead after conversion of units, to a production rate readily observable at Arecibo, if one uses the only value ever derived at Arecibo (Carlson et al, 1982) for conversion efficiency, thus emphasizing the need for further controlled experiments as proposed herein. By way of supporting evidence, following the budget analysis of Carlson (1993), leads for the HAARP experiment testing this, the ERP of 440 MW leads to a power density of 9 x 10-8 W cm-2 at 200 km, which if the efficiency had been 100% produce 2 x 10^{10} ions cm^{-2} s^{-1} for an average energy per ion of 30 eV, integrated over a full column. The observation, taken as integrated over a 20 km thickness, gave 2.9 x 10^{10} ions cm^{-2} s^{-1} which would lead to an efficiency of 10% for an assumed 20 eV/ion (Pedersen et al, 2009) or 15% if 30 eV/ion. Alternately expressed, this is being peak-production of 10^4 ions cm^{-3} s^{-1} , or 2x 10^5 ions cm^{-3} at the production peak in 20 seconds. At Arecibo the power density effects should still be highly measurable with today's new measurement sensitivity.

At HAARP (and Tromso Norway), production of ionization involves the combined effect of upper hybrid heating, consequent formation of striations, subsequent HF ray trapping and extension of HF wave access to altitudes where they can excite parametric instabilities and accelerated electron fluxes and ionization production. Below we note why not all these should apply for Arecibo, hence the need for new experiments for understanding.

5.4 Experimental test Nov 11, 2015

5.4.1 Data collection setup

Now we present the new nighttime PL data collected and processed for simultaneous up/down shifted (down/up going) electrons in the energy range detectable by the radar wavelength at Arecibo (usually < 25eV at night). We used coded long-pulse data taking software [*Sulzer*, 1986] with: a vertical AO line feed to get an antenna gain of 18° K/J (the Gregorian has a sensitivity of 12° K/J at zenith angles below about 18°), a 430 MHz transmitter power of 1.3 MW, and two filter bandwidths of 5MHz upshifted/downshifted by 3.0-8.0 MHz from 430 MHz. The ISR antenna gain, transmitter power monitoring, and calibration pulse were used to place an absolute scale on the PL intensity. The currently upgraded system can get detections in ~10 seconds with ~1kHz and 300 m resolution. The parameters for the new facility are: 600 kW maximum power; gain at 5.1 MHz is between 21.9 and 22.0 dB; the gain at 8.175 MHz is between 25.4 and 25.5.

The geometry of the experiment was as shown in figure 13. At the HF frequency of 5.095 MHz, the HF heater beam was ~10° half power width (for Te deviative absorption heating effects), 10.4° instability zenith angle (ZA) edge (measured by amplitude of HF enhanced PL), so ISR observations were taken at a ZA of 10.8° to view a volume undisturbed by direct HF instabilities.

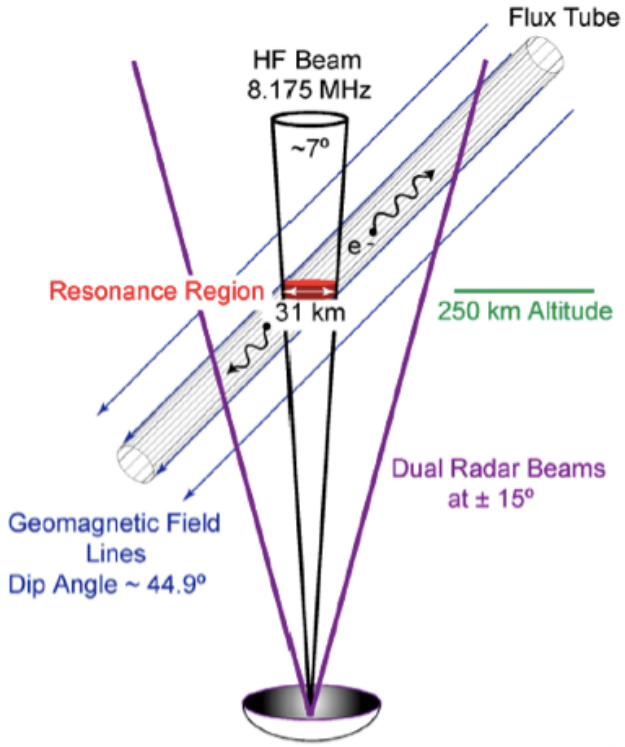

Figure 13: Observing geometry for HF PL experiment. The HF beam is the narrow central cone. The ISR beam measures plasma outside the directly driven instability echo region, to measure Te and PLs excited by HF produced suprathermal electrons. The HF effects propagate up magnetic field lines (**B**) indicated by the blue lines.

5.4 Updating/testing the framework: For the power densities currently at Arecibo we of course do not anticipate ionization production competitive with the sun, but all observations at all HF heating facilities supports the conclusion that AO can generate enough ionization production to test and advance new relevant theory. Some key advances in theory between 1995 and 2001, in partitioning the deposition of significant fractions of radiated HF energy into the ionosphere, included recognition that excitation of upper hybrid (UH) waves led to excitation of plasma striations on scales of ~10 meters found within magnetic field (B) aligned structures (~km transverse to B), grouped into larger patches (summarized in Franz et al, 1999). (1) More quantitatively, in the first step Gurevich, Lukyanov, and Zybin (1995) showed that a steady state of isolated striations developed during ionospheric modification by high power HF radio waves, in which the electron gas would be heated to 2-4 times it's initial thermal value, and electron plasma density (Ne) depletions would saturate at ~2-10%. (2) Because the perturbation in ne is always negative (Gurevich et al, 1998a), this leads to parametric decay of upper hybrid waves becoming trapped inside the ne depletions, self-focusing on striations. It is nonlinear because as the HF pump electric field (Ep) increases, it increases the Ne depletions, further focusing the incident Ep into the depletions, and so on leading to the nonlinear cycle on an increasing number of striations. (3) Focusing increases the effective Ep, which increases the number of striations, producing bunches of striations (Gurevich et al, 1998b), large scale structures 100s m, containing m scale

striations. (4) Because bunches (larger scale structures) have only depleted Ne, HF waves can be trapped (Gurevich et al, 1999). The trapping is most effective only for conditions where the pump HF wave is propagating sufficiently close to parallel to earth's magnetic field B. (5) The geometry of the trapped region was quantified by Gurevich, Carlson and Zybin (2001) to be in an oval region towards magnetic south of the HF transmitter site.

In 2000 exhaustive analysis of Arecibo optical data collected during HF heating operations, was intensively searched for any vestige of southward shifted structure/acceleration. Carlson and Jensen, 2014 showed any southward shift of the optical signature to be undetectable, despite being readily observed at HAARP (Pedersen and Carlson., 2001; Gurevich et al, 2002). This is because Arecibo proceeds only as far as step (3) above, while at high latitudes the conditions proceed through step (5). At high latitudes, significant enhancements of electron fluxes also follow from proximity to multiples of gyro resonances (e.g. Blagoveshchenskaya et al, 2009, Djuth et al, 2005, Gustavson et al, 2006).

5.5 Observations:

The observations presented here (figures 14 and 15) are for November 11, 2015. The data collection system/software was as reported in Carlson et al (2015), used during the first HF heating experiment at Arecibo PR [November 2015] since Hurricane George in September 1998. We present below the first-ever direct comparison of HF produced suprathermal electrons vs. solar EUV produced electrons. The timing of data collection is in local darkness and with a sunlit magnetically conjugate hemisphere. Mantas et al, 1978 has shown the steady state flux from the conjugate hemisphere builds up to about 1.5 times the initial up going "escape" flux from the local sunlit hemisphere. So the flux of solar produced photoelectrons are those incoming from the conjugate hemisphere. In figure 14, the upper frame shows PL excited by only photoelectrons produced by solar EUV {HF transmitter off]. The lower frame with the HF transmitter on has HF suprathermal electrons added. We cycled HF on 2.5 minutes/HF off 2.5 minutes, for a 5-minute cycle (order of a 1° solar zenith angle change). At 19:39 AST the conjugate ionosphere had a 90° solar zenith angle.

Figure 14 shows the PL intensity is comparable for both the HF-accelerated suprathermal and conjugate photoelectrons, clear from simple examination of the raw data. Figure 15 quantifies what the eye can see in figure 14, this with detailed numerical analysis of the digitally recorded data. Figure 15a shows the PL intensity in units of the PL thermal level. Figure 15b, shows the sharp cutoff of the HF suprathermal flux and PL] at the edge of the magnetic flux tubes illuminated by the HF beam. Figure 16 shows the sharp cutoff of HF excitation at the edge of the HF beam, on another representative day on which a satellite pass detailed the characteristic abrupt edge of HF excited instabilities [from above to below threshold HF **E** field excited instabilities].

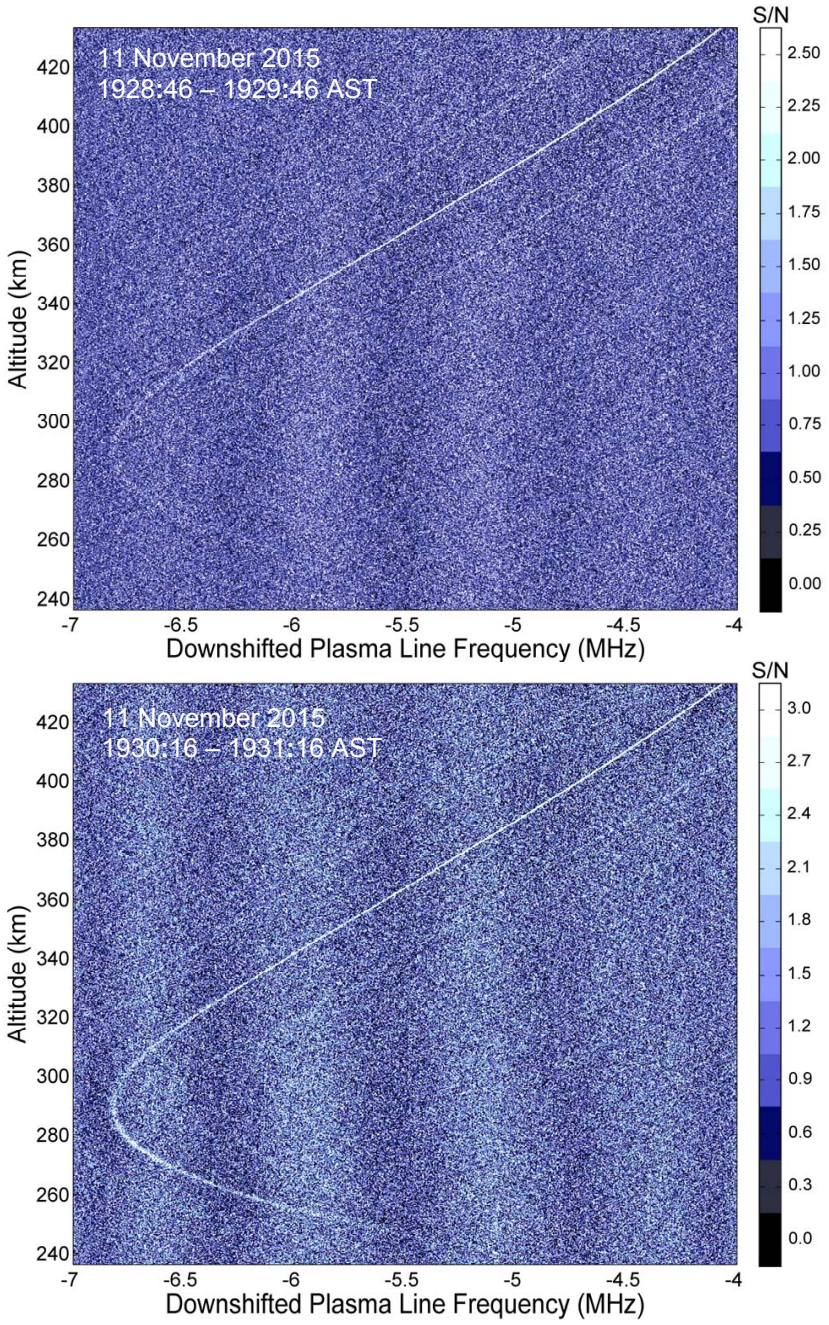

Figure 14: Observed PL intensity where the PL intensity is found to be proportional to conjugate photoelectron flux while the HF heater is off, but its relative intensity in the path of HF excited supra-thermal electrons the PL intensity and flux are comparable. Note particularly the difference between the PL intensity for HF on vs. HF off, between 240 km and 335 km.

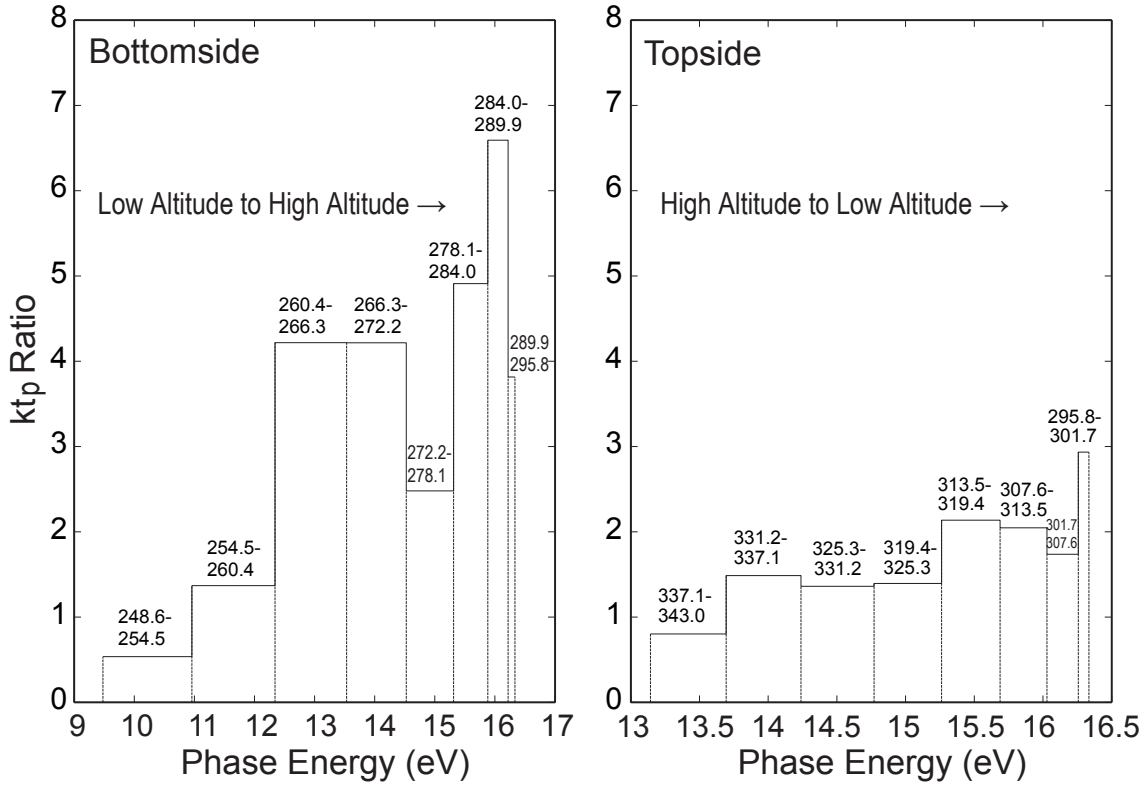

Figure 15 a: Ratio of HF accelerated PL intensity kTp[hf] to kTe in HF projected beam. The HF accelerated-electron PLs are near but less than an order of magnitude greater than kTe.

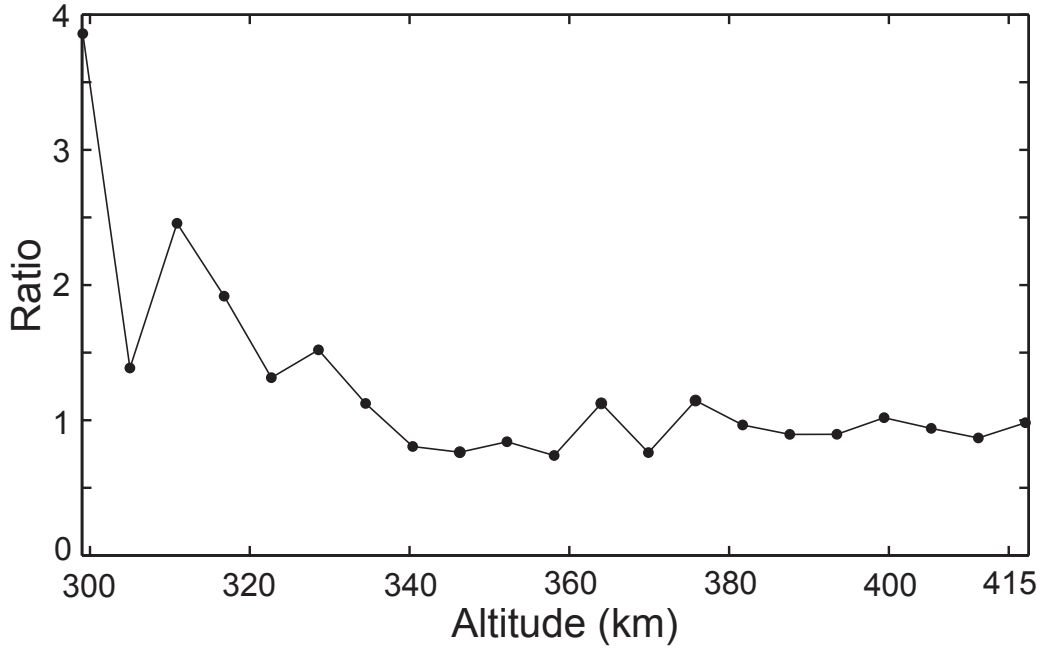

Figure 15 b: Ratio of HF accelerated PL intensity kTp[hf] to kTe at edge and above HF projected beam. Passing across the edge, kTp/kTe ratio falls from ~4 to ~1 +/- ~0.2

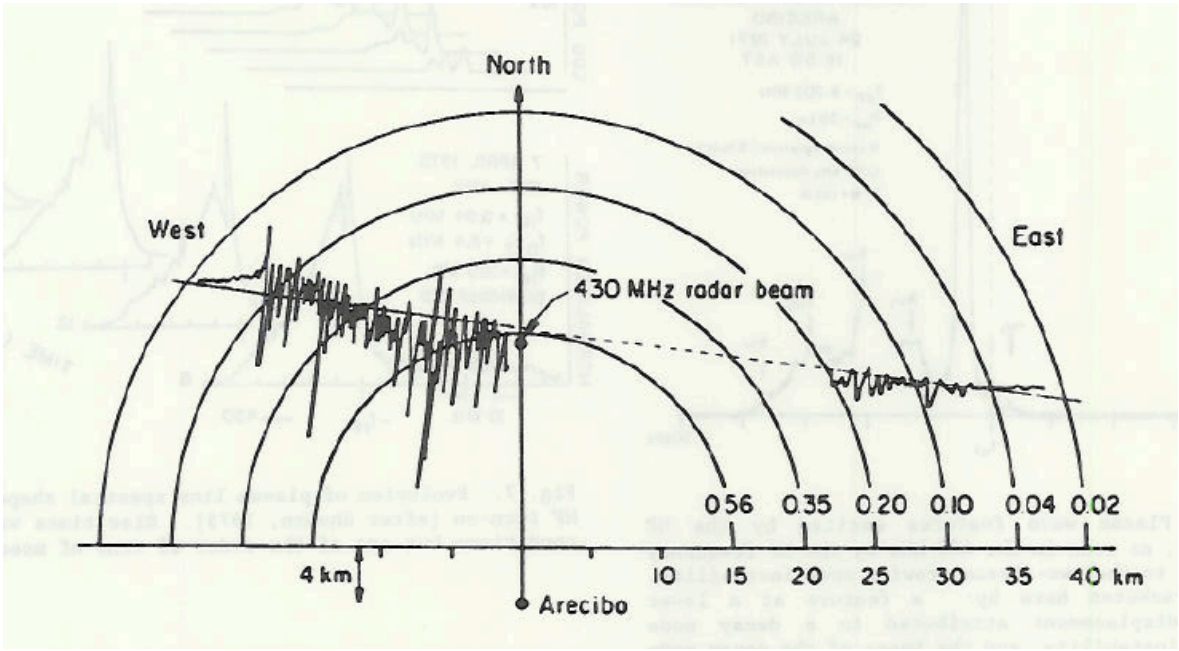

Figure 16: Atmospheric Explorer C satellite pass (15 km north of the Arecibo ISR Observatory) passing through the Arecibo HF heated volume. The sharp boundary edge is apparent on the west end of the measured RPA electron density [Ne] plot, going from very low amplitude fluctuations in Ne [fraction of a %] to sharp several % fluctuations, signature of entry into the HF excited plasma instability region. This shows the sharp onset where the HF intensity exceeds the instability threshold.

The Langmuir wave amplitude is controlled by the amount of time that the photoelectrons spend near the same phase region as the Langmuir wave train; this promotes energy transfer to the Langmuir wave. Thus, the plasma wave intensity depends on the electron velocity distribution function. YP have expressed the energy in the waves in terms of an apparent plasma temperature $T_p(E\phi)$ or intensity $kT_p(E\phi)$ given by:

$$kT_p = kT_e \frac{f_m(E_\phi) + f_p(E_\phi) + \chi}{f_m(E_\phi) - kT_e \dfrac{df_p(E_\phi)}{dE_\phi} + \chi} \qquad (1)$$

where $\mathbf{f}_p$ is the one-dimensional velocity distribution of the photoelectrons along the radar wave vector; $\mathbf{f}_m$ is a modified one-dimensional Maxwellian velocity distribution of the ambient electrons, and chi provides for excitation and damping of plasma waves by the collective effects of electron-ion collisions. $\mathbf{f}_m$ and chi can be readily calculated from the observed values of the electron temperature Te, electron density, the ISR radar look angle relative to the magnetic field B, and radar wavelength.

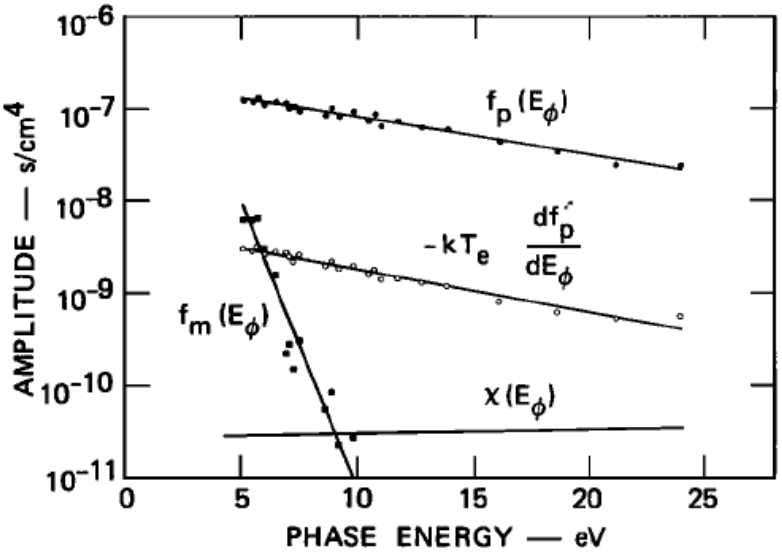

Figure 17: Comparison of theoretical and observed kTp at Arecibo for solar EUV produced photoelectrons (pe), show the self-damping by suprathermal electrons is very small (a few percent) relative to their excitation rate (Carlson et al, 1977). However for the HF excited suprathermal electrons measured here shown in figure 15, the PL intensity and flux are sufficiently small that the self damping term is small relative to the chi thermal damping term so PL intensities lead directly to good estimates of HF suprathermal fluxes themselves.

For the data here Nov 11, 2015 19:30 AST, small self damping reduces equation (1) to:

$$kT_p(E_\phi) = kT_e \left(f_p(E_\phi) + \chi \right) / \chi$$

because f_m is negligible in this phase energy range for this value of Te, and the f_p derivative term in the denominator is much smaller than the collective collision term chi. Thus in contrast to common daytime photoelectron excited PL intensities [e.g. Cicerone et al 1974) which require special computational approaches [Carlson et al, 1977], for cases chosen at times [as here] where the suprathermal flux is clearly measurable but weak, the equations reduce to a form readily solvable in quantitative form [e.g. detailed in Carlson et al, 2015].

Thus kTp near 10-20 eV can be derived here directly from the observed kTp and Te.

Thus the kTp for photoelectrons from solar EUV, as well as for HF suprathermal electrons, are both tracked in this kTp and energy range, by their respective values of kTp/kTe. This is true here through the judicious choice of timing and thus applicable solar zenith angles for solar EUV production relative the HF accelerated electron generation. In short, the figure 14 of PL intensity near equality for solar EUV relative to HF suprathermal excitation, allows the conclusion of near equal suprathermal electron fluxes. For the daytime condition this is not true because of photoelectron self-damping (Carlson et al, 1977), but for our observing time at 19:30 AST tailored to our point here, it is true, just as was the case for the data presented in Carlson et al, 2015.

Because the quantitative values of kTp themselves are close to those of the data from Carlson et al, 1982, and HF energy density levels are comparable, we conclude the %

efficiency found from the initial Arecibo published data, that taken here, and that between these time at HAARP, are all order 10% efficiency. The proposed mechanism is supported whether at high or mid latitudes, despite evidence for different mechanism at the detailed level, this order of energy conversion is supported by the observations.

Therefore: We developed a theoretical framework, performed a unique experiment, did major measurement improvements, and measured comparable HF and solar suprathermal electron production rates, confirming the 1993 prediction. At a more general level, the implication is that, when contrasting the high latitude vs. low latitude experimental data, details of specific conversion mechanism varies but order practical of efficiency is order 10%. If the efficiency were order 1% or less the mechanism would by academic, it cannot be > ~30% simply because no more than ~1/3 of electron impact energy can end up in ionization (references in Carlson and Jensen, 2014).

6. Conclusions

The most significant result of this research is proof that even at mid-latitudes, high power HF radio waves at energy densities approaching that of the sun produce ionization. This is despite the absence of high latitude effects including the "magnetic zenith effect" (Gurevich, Zybin, and Carlson, 2005) and upper hybrid and gyro resonances giving rise to HF trapping and excitation of electron fluxes producing ionization reported at high latitudes (Pedersen et al, 2009, 2010; Blagoveshchenskaya et al, 2009). The physical instability processes are different, so this establishes that it is the HF electric field energy density, not the specific high latitude processes, that are the critical factor. Sufficiently intense rf energy density will generate processes in the plasma that ultimately dissipate energy in the form of accelerating electrons, a very effective mechanism for transporting energy out of the energy deposition region.

The generalization suggested is that above some realizable energy density threshold, the key is to view accelerated electrons as an essential way to transport significant energy out of the HF energy deposition volume. Several possible processes are already identified, but it may be less important precisely which process dominates under which conditions, and more important to determine the net fraction of energy which through some ensemble of processes will end up carried away as accelerated electrons. i.e. focus on the net energy balance and partitioning.

Several *other* important findings have also been published and presented at workshops, meetings, and given as invited talks.

The observations we present here were at several wavelengths to see how comparison of observation at different energy thresholds could illuminate knowledge of the spectra. This much is not new, the field has even moved on to as many as five wavelengths (e.g. Hysell 2014) to pursue such goals. What is new from our analysis here, including comparison of observations with aeronomical model runs (Carlson et al. 1982), sheds new light on past and future data collection goals, and analysis techniques (Carlson and Jensen, 2014).

Further important conclusions include:

A) We have shown that inclusion of suprathermal electron energy loss for energies below 10 eV, is an important consideration to include when the goal of the research is to combine observation of 557.7 nm emissions with higher energy threshold emissions (e.g. 777.4, 844.6, 427.8, etc.) in order to estimate or experimentally constrain/guide future theory and modeling of HF accelerated suprathermal electron fluxes. This particularly relates to issues with HF production of artificial ionospheres.

B) For past and future data: The altitude differences in observed electron impact excited optical emissions can make a valuable observational contribution to and constraint on understanding the essential transport part of the overall interpretation. However to realize this potential, account needs to be taken of losses of the component of electron flux below 10 eV, where electron densities/content can be a reasonable fraction of daytime values.

C) For future observations: (a) The geometry of the Arecibo magnetic field makes direct observations overhead the HF heater valuable to trace from the acceleration source altitude to the different center-of-gravity stopping altitudes for different optical wavelengths emissions. This observational differentiation is of value to interpretation. It significantly mitigates the observational loss when side-looking optics is absent, and compliments the added value when present and (b) one should make coincident measurements of the altitude profile of electron density.

D) We continue to find most fruitful, the framework developed under this grant, of separating the problem of production of an artificial ionosphere into three parts:

1. Deposition of HF energy into the ionosphere with effectiveness.
2. Acceleration of electrons by instability processes, including multiple plasma resonances.
3. Transport of accelerated electrons from HF-interaction region to plasma-production region.

7. Supplementary information

Student accomplishments: Joseph B. Jensen earned co-authorship (to be his first publication in a reviewed journal) of a paper submitted for publication "HF accelerated electron fluxes, spectra, and ionization" by H. C. Carlson and J. B. Jensen, based on his significant accomplishments and contributions to the work he did while at the USU as a senior in the Physics Department. During the past year he has taken the 7 modules from the 1970s, recompiled them, and under the guidance of the PI on the grant reported upon herein, has collaboratively gone through every module to bring it into good working order. He has input EVE EUV data to test and verify the program modules 1-3, for yielding photoelectron production rates and calculating photoelectron fluxes at altitudes separated by fractional neutral scale height intervals, and with the PI checked outputs/inputs sequentially up through and including transformation of the photoelectron fluxes into equivalent incoherent scatter plasma line intensities, as required for work on this grant. He has performed these tasks while maintaining a GPA of 3.75, graduating cum laude. This highly skill, motivated, and accomplished young scientist has gone on after graduation to stay in tour field, and shows high promise to become a shining star within the space sciences community. He is now a graduate student working towards his PhD at the Physics Dept., University of New Hampshire, Durham, NH

Other accomplishments: The PI on this grant has given an invited lecture, which was the opening talk in the 1.5 day special session on 40th COSPAR Scientific Assembly entitled: "HF Radio Wave Production of Artificial Ionospheres". He has also published a paper (Carlson and Jensen, 2014) reporting discovery of important changes that must be made by the community in its enhanced efforts to test HF accelerated electron energy spectra using the most readily available mans- optical emission line intensities. We applied models of electron transport and impact excitation, to demonstrate theoretically that one of the most commonly used lines (557.7 nm) for such purposes, must be corrected for energy losses to the ambient electron gas. We furthermore also experimentally verified this. The correction can be half an order of magnitude, and is thus major. The PI accepted an invitation to serve as a committee member of the National

Academy of Sciences/NRC study “High-Power High-Frequency Transmitters to Advance Ionospheric Thermospheric Research”. The broad motivational figure 3 of that report (NAS ISBN 978-0-309-29859-9, 2014), which is also figure 1 of this AFOSR final report, was reproduced from Carlson, 1993. The PI also accepted the invitation to give two invited talks at the 2016 annual RF Ionospheric–Interactions Workshop, featuring results from research under this grant.

Work under this grant, and also described in this report, has also been given as two invited papers at the Radio Frequency Interactions Workshop, Santa Fe NM, 2015.

References:

V.J. Abreu, H.C. Carlson, J. Geophys. Res., 82, 1017-1023 (1977)
P.A. Bernhardt, C.A. Tepley, L.M. Duncan, J. Geophys. Res., 94, 9071–9092 (1989)
N.F. Blagoveshchenskaya, H.C. Carlson, V.A. Kornienko, T.D. Borisova, M.T. Rietveld, T.K. Yeoman, A. Brekke, Ann. Geophys., 27, 131–145 (2009)
H.C. Carlson, Artificial ionosphere-Creation using high power HF transmitters, AFGL1987/ILIR7L, AFGL(PL/CAG), Hanscom AFB, MA, 01731 (1987)
H.C. Carlson, Adv. Space Res., 13, 1015-1024 (1993)
H.C. Carlson, Proceedings HG3 Ionospheric modification by high power radio waves: coupling of plasma processes, URSI General Assembly, Lille France (1996)
H.C. Carlson, V.B. Wickwar, G.P. Mantas, J. Atmos. Terr. Phys., 44, 1089-1100 (1982)
H.C. Carlson, W.E. Gordon, R.L. Showen, J. Geophys. Res., 77, 1242-1250 (1972)
H.C. Carlson, V. B. Wickwar, and G. P. Mantas (1977), The plasma line revisited as an aeronomical diagnostic: suprathermal electrons, solar EUV, electron-gas thermal balance, Geophys. Res. Lett., 4, 565-567.
Carlson, H. C., and J. B. Jensen, 2014, HF Accelerated electron fluxes, spectra, and ionization, Earth Moon Planets, Springer, DOI 10.1007/s11038-014-9454-6.
R. J. Cicerone, (1974), Photoelectrons in the ionosphere: Radar measurements and theoretical computations, Rev. Geophys. Space Phys., 12, 259.
R. J. Cicerone, W. E. Swartz, R. S. Stolarski, A. F. Nagy, and J. S. Nisbet (1973), Thermalization and transport of photoelectrons: A comparison of theoretical approaches, J. Geophys. Res., 78, 6709-6719.
A. Dalgarno and G. Lejeune (1971), The absorption of electrons in atomic oxygen, Planet. Space Sci., 19, 1653.
F.T. Djuth, T.R. Pedersen, E.A. Gerken, P.A. Bernhardt, C.A. Selcher, W.A. Bristow, J.H. Kosch, Phys. Rev. Lett., 94, 125001 (2005)
B. Eliasson, X. Shao, G.M. Milikh, E.V. Mishin, K.D. Papadopoulos, J. Geophys. Res., 117, A10321, (2012)
J. W. Evans, (1969), Theory and practice of ionosphere study by Thomson scatter radar, Proc. IEEE, 57, 496.
J.A. Fejer, Geophys Res. Lett., 4(7), 289-290 (1977)
J.A. Fejer, (1979), Rev. Geophys.1, 7, 135-
153 (1979) P.A. Fialer, Radio Sci., 9 (1974)
J.L. Fox, M.I. Galand, R.E. Johnson, Space Sci. Rev., 136; 3-62 (2008)
Franz, Kelley, and Gurevich, Radio Sci, 34, 465-475, 1999
Y. Gong, Z. Qihou, Z. Shaodong, N. Aponte, M. Sulzer, S. Gonzalez, J. Geophys. Res., 117, A08331 (2012)
W.E. Gordon, R.L. Showen, H.C. Carlson, J. Geophys. Res., 76, 7808-7813 (1971)
A.V. Gurevich, Usp. Fizicheskikh Nauk., 177(11), 1145–1177 (2007)
A.V. Gurevich, Y.A. Dimant, G.M. Milikh, V.V. Vaskov, J. Atmos. Terr. Phys., 47, 1057-1070 (1985)
A, V, Gurevich, Zybin K. P. and Lukyanov, A. V., Phys. Rev. Lett., 75, 2622, (1995).

A. V. Gurevich, Carlson, H. C., Lukyanov, A.V. and Zybin, K.P., Parametric decay of upper hybrid plasma waves trapped inside density irregularities in the ionosphere, Phys. Lett. A, 231, 97-108, 1997.
A. V. Gurevich, T. Hagfors, H. C. Carlson, Karashin, A. and Zybin, K.P., Self-Oscillations and bunching of striations in ionospheric modifications, Phys. Lett. A, 239, 385-392, 1998.
A. V. Gurevich, Carlson, H.C., Kelley, M., Hagfors, T., Karashtin, A. and Zybin, K., Nonlinear Structuring of the ionosphere modified by powerful radio waves at low latitudes, J. Physics Lett. A 251, 311-321, 1999.
A.V. Gurevich, H.C. Carlson, G.M. Milikh, K.P. Zybin, F.T. Djuth, K. Groves, Geophy. Res. Lett., 27, 2462-2464 (2000)
A.V. Gurevich, H.C. Carlson, K.P. Zybin, Phys. Lett. A., (2001)
A.V. Gurevich, K.P. Zybin, H.C. Carlson, T. Pedersen, Phys. Lett. A, 305, 264-274 (2002)
A.V. Gurevich, H.C. Carlson, Y.V. Medvedev, K.P. Zybin, Plasma Phys. Rep., 30 (12), 995–1005 (2004)
A.V. Gurevich, K.P. Zybin, H.C. Carlson, Radiophys. Quantum Electron. (Engl. Transl.), 48, 9 (2005)
B. Gustavsson, et al., Ann. Geophys., 23, 1747–1754 (2005)
B. Gustavsson, Lyser, Kosch, et al, Phys. Rev. Lett, 97, 195002, 2006.
B. Gustavsson and B. Eliasson, J. Geophys. Res., 113, A08319, (2008)
J.C. Haslett, L.R. Megill, Radio Sci., 9, 1005–1019 (1974)
D.L. Hysell, R.H. Varney, M.N. Vlasov, E.Nossa, B. Watkins, T. Pedersen J.D. Huba, J. Geophys. Res., 117, A02317 (2012)
D.L. Hysell, R.J. Miceli, E.A. Kendall, N.M. Schlatter, R.H. Varney, B.J. Watkins, T.R. Pedersen, P.A. Bernhardt, J.D. Huba, J. Geophys. Res. Space Phys., 119, 2038–2045 (2014)
Y. Itikawa, J. Phys. Chem. Ref. Data, 35, No 1 (2006)
K.S. Kalogerakis, T.G. Slanger, E.A. Kendall, T.R. Pedersen, M.J. Kosch, B. Gustavsson, M.T. Rietveld, Ann. Geophys., 27, 2183–2189 (2009)
M. Kelly, Arce, et al, JGR, 100, p17367-17376,1995
M.J. Kosch, M.T. Rietveld, T. Hagfors, T.B. Leyser, Geophys. Res. Lett., 27, 2817-2820 (2000)
G. P. Mantas, H. C. Carlson, C. LaHoz, J. Geophys. Res., 86, 561-574 (1981)
G. P. Mantas, (1973), Electron collision processes in the ionosphere, Ph.D. thesis, Univ. of Ill., Urbana.
G. P. Mantas, (1975a), Theory of photoelectron thermalization and transport in the ionosphere, Planet Space Sci., 23, 337-352.
G. P. Mantas, V. B. Wickwar and H. C. Carlson (1975b), Plasma line and theoretical studies of photoelectrons at Arecibo, Trans. A.G.U., 56, 1037.
G. P. Mantas, H. C. Carlson, and V. B. Wickwar (1978), Photoelectron flux build-up in the plasmasphere, J. Geophys. Res., 83, 1-15.
C.K. Mutiso, J.M. Hughes, G.G. Sivjee, T. Pedersen, B. Gustavsson, M.J. Kosch, Geophys. Res. Lett., 35, L14103 (2008)
T.R. Pedersen, H.C. Carlson, Radio Sci., 36, 1013-1026 (2001)
I. R. Pedersen, M. McCarrick, E. Gerkin, C. Selcher, D. Senteman, H. C. Carlson, and A. Gurevich, (2003), Magnetic zenith enhancement of HF radio-enhanced airglow production at HAARP, Geophys. Res. Lett., 30(4), 1169, doi:10.1029/2002GL016096.GUREVICH

T.R. Pedersen, B. Gustavsson, E. Mishin, E. MacKenzie, H.C. Carlson, M. Starks, T. Mills, Geophys. Res. Lett., 36, L18107 (2009)
T. Pedersen, B. Gustavsson, E. Mishin, E. Kendall, T. Mills, H.C. Carlson, A.L. Snyder, Creation of artificial ionospheric layers using high-power HF waves, Geophys. Res. Lett., 37, L02106 (2010)
F.W. Perkins, C. Oberman, E.J. Valeo, J. Geophys. Res., 79, 1478-1496 (1974)
F. W. Perkins and E. E. Salpeter (1965), Enhancement of plasma density fluctuations by non-thermal electrons, Phys. Rev., 139, A55-A62.
A. V. Pavlov, (1998a), New electron energy transfer and cooling rates by excitation of O2, Ann. Geophysicae, 16, 1007.
A. V. Pavlov, (1998b) New electron energy transfer and cooling rates for vibrational excitation of N2, Ann. Geophysicae, 16, 176.
A. V. Pavlov and K. A. Berrington (1999), Cooling rate of thermal electrons by electron impact excitation of fine structure levels of atomic oxygen, Ann. Geophysicae, I 7, 919.
M.H. Rees, R.G. Roble, Rev. Geophys., 13, 201–242 (1975)
M.H. Rees, R.G. Roble, Can. J. Phys., 64, 1608 (1986)
H. Rishbeth and O. K Garriott, Introduction to Ionospheric Physics, Academic Press, NY, 1969
G. Rose, B. Grandal, E. Neske, W. Ott, K. Spenner, J. Holtet, K. Måseide, J. Trøim, J. Geophys. Res., 90, 2851–2860 (1985)
R.W. Schunk, P.B. Hays, Planet. Space Sci., 19, 113 (1971)
R. W. Schunk and A. Nagy (2009), Ionospheres: Physics, Plasma Physics, and Chemistry, Tables 9.3 and 9.4, Cambridge University Press, NY, ISBN 978-0-521-87706-0.
T. Sergienko, B. Gustavsson, U. Bringstrom, K. Axelsson, Geophys., 30, 885-895 (2012)
W. Simon, C., G. Gronoff, J. Lilensten, H. Ménager, M. Barthélemy, Ann. Geophys., 29, 187-195 (2011)
D. P. Sipler, M.A. Biondi, J. Geophys. Res., 77, 6202-6212 (1972)
D. J. Strickland, J.R. Jasperse, J.A. Whalen, J. Geophys. Res., 88, 8051 (1983)
M. P. Sulzer, (1986), A radar technique for high range resolution incoherent scatter autocorrelation function measurements utilizing the full power of klystron radars, *Radio Sci.*, *21*, 1033-1040.
W.F. Utlaut, R. Cohen, Science, 174, 245-254 (1971)
J. Weinstock, Radio Sci., 9, 1085-1087 (1974)
K. O. Yngvesson and F. W. Perkins (1968), Radar Thomson scatter studies of Photoelectrons in the ionosphere and Landau damping, J. Geophys. Res., 73, 97-1

1.

1. Report Type

Final Report

Primary Contact E-mail
Contact email if there is a problem with the report.

herbert.c.carlson@gmail.com

Primary Contact Phone Number
Contact phone number if there is a problem with the report

435-760-1831

Organization / Institution name

Utah State University, CASS,

Grant/Contract Title
The full title of the funded effort.

creating space plasmas from the ground

Grant/Contract Number
AFOSR assigned control number. It must begin with "FA9550" or "F49620" or "FA2386".

FA9550-11-1-0236

Principal Investigator Name
The full name of the principal investigator on the grant or contract.

Herbert Carlson

Program Manager
The AFOSR Program Manager currently assigned to the award

Julie Moses

Reporting Period Start Date

08/14/2012

Reporting Period End Date

05/14/2016

Abstract

It was predicted (Carlson, 1987; 1993) that once HF radio waves achieved ionospheric energy densities comparable to that from the solar EUV, they could produce their own ionosphere. That work estimated a GW ERP of rf energy would produce an ionosphere half that from an overhead sun, assuming ~15% efficiency conversion of rf energy to accelerated electron energy. [Until 2009 only one experimental estimate existed, ~15% from Carlson, 1982.] The production mechanism proposed was impact ionization, by HF-accelerated electrons, to energies exceeding thermospheric ionization potentials. Solar EUV, aurora, and high-power HF radio-waves produce suprathermal electrons in the 15-100 eV energy range, yielding long-lived ionization in the ionosphere. Once suprathermal electrons are produced, the Aeronomy of production, transport, and recombination are in common. The key to understanding artificial ionization thus reduces to conversion efficiency of HF energy to ionization. By 2008 technology reached ~GW ERP. The prediction was tested, and confirmed [Pedersen et al, 2009, Blagoveschenskaya et al, 2009] at high latitudes. However, confirmation was at only high latitudes, and by then new theory [Gurevich, Zybin, and Carlson, 2005] had shown multiple physical processes conspire to significantly amplify high latitude suprathermal electron production. To test if the prediction was therefore invalidated at mid-latitudes, we performed a definitive test at Arecibo in November 2015, its first HF operation since Hurricane George in 1998. We developed a theoretical framework, performed a unique experiment, did major improvements in

measurements, and measured comparable HF and solar suprathermal electron production rates, thereby confirming the 1993 prediction.

Distribution Statement

This is block 12 on the SF298 form.

Distribution A - Approved for Public Release

Explanation for Distribution Statement

If this is not approved for public release, please provide a short explanation. E.g., contains proprietary information.

SF298 Form

Please attach your SF298 form. A blank SF298 can be found here. Please do not password protect or secure the PDF The maximum file size for an SF298 is 50MB.

AFD-070820-035.pdf

Upload the Report Document. File must be a PDF. Please do not password protect or secure the PDF . The maximum file size for the Report Document is 50MB.

AFOSR Final Report 2016 d FINAL.pdf

Upload a Report Document, if any. The maximum file size for the Report Document is 50MB.

Archival Publications (published) during reporting period:

Carlson, H. C., and J. B. Jensen, 2014, HF Accelerated electron fluxes, spectra, and ionization, Earth Moon Planets, Springer, DOI 10.1007/s11038-014-9454-6.

Changes in research objectives (if any):

none

Change in AFOSR Program Manager, if any:

from Dr. Kent Miller to Dr. Julie Moses

Extensions granted or milestones slipped, if any:

Extension granted from August 14, 2015 to Feb 14 2016

AFOSR LRIR Number

LRIR Title

Reporting Period

Laboratory Task Manager

Program Officer

Research Objectives

Technical Summary

Funding Summary by Cost Category (by FY, $K)

	Starting FY	FY+1	FY+2
Salary			
Equipment/Facilities			
Supplies			
Total			

Report Document

Report Document - Text Analysis

Report Document - Text Analysis

Appendix Documents

2. Thank You

E-mail user

May 07, 2016 14:55:00 Success: Email Sent to: herbert.c.carlson@gmail.com